Journal Pre-proof

Breaking the boundaries in spectrometry. Molecular analysis with atomic spectrometric techniques

M. Resano, M. Aramendía, F.V. Nakadi, E. García-Ruiz, C. Alvarez-Llamas, N. Bordel, J. Pisonero, Eduardo Bolea-Fernández, Tong Liu, Frank Vanhaecke

PII: S0165-9936(20)30184-9

DOI: https://doi.org/10.1016/j.trac.2020.115955

Reference: TRAC 115955

To appear in: *Trends in Analytical Chemistry*

Received Date: 15 February 2020

Revised Date: 31 March 2020

Accepted Date: 5 June 2020

Please cite this article as: M. Resano, M. Aramendía, F.V. Nakadi, E. García-Ruiz, C. Alvarez-Llamas, N. Bordel, J. Pisonero, E. Bolea-Fernández, T. Liu, F. Vanhaecke, Breaking the boundaries in spectrometry. Molecular analysis with atomic spectrometric techniques, *Trends in Analytical Chemistry*, https://doi.org/10.1016/j.trac.2020.115955.

Breaking the boundaries in spectrometry. Molecular analysis with atomic spectrometric techniques

M. Resano[a*], M. Aramendía[b], F.V. Nakadi[a], E. García-Ruiz[a], C. Alvarez-Llamas[c], N. Bordel[d], J. Pisonero[d], Eduardo Bolea-Fernández[e], Tong Liu[e], Frank Vanhaecke[e]

[a]Department of Analytical Chemistry, Aragón Institute of Engineering Research (I3A), University of Zaragoza, Pedro Cerbuna 12, 50009, Zaragoza, Spain. E-mail: mresano@unizar.es

[b]Centro Universitario de la Defensa de Zaragoza, Carretera de Huesca s/n, 50090, Zaragoza, Spain

[c]UMALASERLAB, Department of Analytical Chemistry, University of Málaga, C/Jiménez Fraud 4, Malaga 29010, Spain

[d]University of Oviedo, Faculty of Science, Department of Physics C/ Federico García Lorca 18, 33007 Oviedo, Spain

[e]Ghent University, Department of Chemistry, Atomic & Mass Spectrometry e A&MS Research Unit, Campus Sterre, Krijgslaan 281-S12, 9000, Ghent, Belgium

Abstract

Since the development of atomic spectrometry, trace element and isotopic analysis has been mainly based on the monitoring of atomic spectra and monoionic species. However, according to the literature and considering the current instrumental developments, it seems that some of the remaining challenges in this field can be mitigated *via* the measurement of molecular spectra or of polyatomic ions. This review discusses recent advances in three of the most important atomic techniques (laser-induced breakdown spectrometry, high-resolution continuum source atomic absorption spectrometry and inductively coupled plasma mass spectrometry) and how the monitoring of such molecules or polyatomic ions containing the target analyte enables attaining better selectivity and opens new ways to determine non-metals and to obtain isotopic information.

Keywords: trace elemental analysis; determination of non-metals; isotopic analysis; laser-induced breakdown spectrometry; laser ablation molecular isotopic spectrometry; high-resolution continuum source atomic/molecular absorption spectrometry; tandem inductively coupled plasma mass spectrometry; molecular ion monitoring.

1. Introduction. Problems remaining in elemental analysis.

For many years, there has been a division in analytical spectroscopy between molecular and atomic spectrometry, which were considered as two branches that were separating away. Indeed, the instruments developed for atomic spectrometry, with the obvious need for vaporization, atomization and, sometimes, even ionization, were very different from those used for molecular spectrometry, and the spectra observed in both cases also differed significantly. Nowadays, however, such division needs to be reevaluated, since there are various types of works that are linking these two branches.

Leaving aside the use of hyphenated techniques and the development of indirect methods, which is after all not so uncommon in other areas of Analytical Chemistry, we would like to point the attention to the increasing number of works carried out with atomic sources that are evaluating the measurement of molecular species in order to obtain elemental or isotopic information of superior quality. This fact has been recognized by *Journal of Analytical Atomic Spectrometry* in an editorial, in which the Journal has clarified its scope widening it and including new types of works: articles in which atomic techniques are deployed but with the purpose of attaining molecular information, and those articles targeting molecular species using atomic sources but with the goal to obtain elemental or isotopic analysis [1].

This article reviews the last situation, which is in principle more paradoxical, as one of the reasons behind the development of methods based on the measurement of atoms or of atomic ions was the production of much simpler spectral information, eventually leading to a higher selectivity, which, depending on the source used for atomization/ionization, was also accompanied by excellent sensitivity. Trace element analysis has been cemented on this principle. However, it is becoming clearer that

the measurement of molecular species opens new possibilities to address some of the most challenging issues remaining today in elemental and isotopic analysis.

The reason for this is mostly related with all the recent instrumental developments, which have significantly improved the spectral resolution attainable, as well as the detection capabilities. It is not so obvious, for instance, that if the “rediscovery” of atomic absorption by A. Walsh was occurring today a line source would still be proposed over a continuum one, simply because the use of the former required spectrometers of much lower resolution [2,3]. Some traditional limitations are simply not valid anymore, and thus, the monitoring of molecular species is being reexamined using state-of-the-art “atomic” instrumentation, leading to the development of methodologies of great novelty and value. Perhaps the two most prominent examples are related with the determination of non-metals and with isotopic analysis.

Indeed, the determination of non-metals (such as Br, Cl, F, I, N, P or S) is either very challenging for most atomic techniques, or even impossible in some cases. Besides several practical problems related to sample preparation, the high electronic affinity of these elements results in a high energy required to promote any electronic transition or to ionize these atoms. As a result, their main atomic absorption/emission lines fall in the vacuum ultraviolet (VUV) region, difficulting their determination by optical techniques, while the high ionization potential, in combination with the occurrence of spectral overlap, hampers their determination by inductively coupled plasma mass spectrometry (ICP-MS). However, it will be discussed in this review how the generation and measurement of molecules or of polyatomic ions containing the analyte may result in significant improvements for trace determination of these elements by means of these techniques [4,5].

Isotopic analysis is another field that can benefit from the approach discussed in this review. This field practically relies only on mass spectrometry techniques. It is well-known that atomic lines also show isotopic shifts, but these are often too small to enable the proper independent quantification of the different isotopes involved in these transitions. However, the isotopic shifts reported for molecules are often much larger than those observed for atoms. Therefore, if molecules containing the analyte are formed and targeted with optical techniques, then it becomes feasible to obtain isotopic information also [6]. And the formation of polyatomic ions may also help in alleviating common spectral interferences when using ICP-MS for isotopic analysis.

This review will examine how the monitoring of molecular spectra or polyatomic ions enables obtaining information that is not possible to attain easily *via* the measurement of atoms or atomic ions, leading to: i) an improved selectivity for challenging elements; ii) new possibilities for the determination of non-metals at trace levels, and iii) isotopic information. And to further show that this is a general trend not associated only with one technique, three very popular (if not the most popular) atomic techniques have been selected to illustrate this principle. Namely, laser-induced breakdown spectroscopy (LIBS), atomic absorption spectrometry (using high-resolution continuum source devices, HR CS AAS), and ICP-MS.

2. Molecular analysis using optical atomic sources: Molecular emission spectrometry in laser induced plasmas.

2.1. Laser-induced breakdown spectroscopy. A short introduction.

LIBS is an analytical technique based on the measurement of the emitted radiation coming from a laser induced plasma created after the irradiation of a sample by a short duration laser pulse (usually in the order of nanosecond or below). The

instrumentation required to obtain an appropriate signal from the interrogated sample is based, in a general way, on a pulsed laser with enough fluence (energy per unit of area) to initiate the ablation process (the typical values are in the order of 1-10 J cm^{-2}, with laser energies of 10^{-4}-1 J per pulse, and pulse widths of 10^{-15}-10^{-9} s), a combination of common optical components (lenses, mirrors…) to focus the incoming/outcoming radiation, and a spectrometer (being Czerny-Turner or Echelle the most usual configurations) coupled to a detector to collect and analyze the plasma radiation (typically a CCD type) detector. Although the basic instrumentation required to acquire a spectrum from the sample is not complex, obtaining optimal spectroscopic signals for specific elements and/or samples can require more sophisticated equipment (specific optical devices; time-resolved spectrometers with high spectral resolution; ablation chambers, particular gas atmospheres, etc.) as well as an accurate optimization of the experimental parameters [7,8].

LIBS enables fast analysis of samples of any physical state (solid, liquid, gas, or aerosol) with none or minimum sample pre-treatment. Furthermore, LIBS allows in-situ analysis (e.g. portable LIBS) and stand-off measurements. On the other hand, LIBS typically shows strong matrix effects, which constitute one of its main drawbacks when aiming at quantitative information. Another weakness of LIBS is related to its lower repeatability in comparison with other analytical technique such as ICP-MS or AAS.

Most of the LIBS applications are based on the use of atomic emission, mainly coming from neutral and first ionized elemental excited species in the plasma; however, the analysis of the emission produced by excited molecules present in the plasma can improve the analytical capabilities of the technique for specific cases, opening new roads in LIBS fields of application. The feasibility of detecting the

emission from the molecular species in LIBS plasma has been shown since the early times of the technique [9].

Molecular creation mechanisms, in a typical LIBS plasma, are very complex issues still under investigation. In general, molecules in LIBS plasmas can be formed following two main routes: recombination processes, and fragmentation processes. As it is known, after the interaction between the laser and the sample, its constituents are atomized, ionized, and excited in the plasma. These species can undergo recombination processes, creating small molecules. During the plasma expansion, the components of the environment become part of the plasma, also reacting and/or recombining with other plasma species giving rise to new molecules. In the ablation of molecular solids, part of the target molecules might be partially fragmented, and once in the plasma undergo substitution reactions or further fragmentations into smaller molecules [10,11]. The prevalence of some specific mechanisms versus others in the molecular production depends on the experimental conditions, and on parameters such as the kind of molecular solids, the environment surrounding the sample, the laser pulse duration or the laser energy.

De Giacomo and Hermann [12] described the initial evolution (e.g. first microseconds) of a laser induced plasma generated by a ns laser, as an atomic dominated plasma due to the high temperatures (tens of thousands of kelvin) and high electron densities ($>10^{17}$ cm^{-3}) conditions. Subsequent molecular formation and excitation in the plasma take place when a critical density of the atomic reagents that form the molecule (either within the plasma, or in the plasma/ambient exchange zone) is reached, and when an adequate temperature range is achieved to allow for electronic excitation but not to produce molecular dissociation. In this sense the stability of the molecules in the plasma is directly related with their dissociation

energy, D_0. Molecules with high D_0 values, >6 eV (e.g. CO, BO, NO,…) can exist even at the first stages of the plasma formation, while molecules with low D_0 (<3 eV) are formed when plasma temperatures significantly decrease; in consequence, their excited electronic states cannot be populated and these molecules are hardly observable (e.g. CuO, AuO,…). Molecules with D_0 values in the intermediate range (e.g. CaF, CaO, …) can be observed at longer delay times where plasma temperature is reduced but population of excited electronic states is still achievable.

It can be highlighted that molecular emission can be observed at very short delay times (hundreds of ns) due to the fragmentation of larger molecules in smaller parts after ablation [13]. However, independently of the type of molecule or processes involved in its generation, the detection of the molecular emission for LIBS applications is favored at long delay times, either to permit molecule formation, or to minimize the spectral interferences from the atomic/ionic excited species, whose emission decay faster.

Considering the possibilities offered by the measurement of molecular emission in LIBS, the following paragraphs describe two methodologies, or approaches, that provide a significant improvement of the analytical characteristics of this technique: the determination of halogens and other non-metals using molecular emission bands, and the isotopic analysis using LIBS, which is usually denominated LAMIS (laser ablation molecular isotopic spectrometry).

2.2. Molecular LIBS for the determination of non-metals

It is known that the determination of some non-metallic elements such as Br, Cl, F, I, P or S by optical emission spectroscopy, and therefore by LIBS, is a difficult issue. As mentioned in the Introduction, the resonance lines of these elements are in VUV

region and the detection of these lines requires the use of reduced pressure in different atmosphere compositions or purged chambers for the ablation, as well as adapting the optical detection systems at these conditions. Alternatively, non-resonance emission lines with wavelengths in the visible near-infrared region (VIS-NIR) can be selected to carry out LIBS analysis. However, these lines show low relative intensities, thus providing low sensitivities and high detection limits when using a typical LIBS instrument. It is also possible to find emission of ionized elements in the VIS spectral region, but the high ionization energy, greater than 10 – 17 eV for these elements, greatly hampers their determination.

To overcome these limitations, different approaches were described in the literature, some of them being based on the combination of several techniques to enhance the excitation of these elements with a secondary excitation source after the ablation: LIBS-LIF [14] (i.e. excitation to a given state of specific atoms or molecules present in the laser induced plasma using a second laser with tunable wavelength to detect its subsequent spontaneous emission), GD-LIBS [15] (i.e. re-excitation of the ablated species using a glow discharge placed close to the laser induced plasma) or double pulse LIBS [16] (i.e. increase of LIBS emission signal by using a second consecutive laser pulse with an optimized delay between them). Nevertheless, the strategy most often deployed consists in measuring the NIR lines emitted by the plasma generated in a Helium atmosphere. The results showed that higher signal to background ratios are achieved. One of the first works published following this methodology studied the detection of fluorine and chlorine in gas phase showing a great improvement of the detection limits of these elements (more than 1 and almost 3 orders of magnitude for Cl and F, respectively) [17-26].

Another approach based on the detection of emission bands emitted by molecules formed by the element of interest and a metallic element was recently reported. Related publications were mainly focused on the determination of fluorine and chlorine, showing noticeable decreases in the detection limits in comparison to the ones obtained when elemental signals were used. It should be highlighted that the detection of the molecular emission bands emitted from diatomic molecules formed by calcium and a halogen was already used for a long time in spectroscopy to improve the spectroscopic sensitivity for the halogens. For instance, CaF molecular emission was already observed at the beginnings of modern spectroscopy. In 1921, Datta and Fowler showed a series of spectra taken using spark spectroscopy for various calcium-fluorine compounds [27]. This work also referred to measurements of CaF_2 bands published in 1864 by M. Mitscherlich. So, it seems that the optical detection of CaF emission has been carried out in optical spectroscopy for more than 150 years. Furthermore, the use of the CaF emission bands for the estimation of the quantity of fluorine in samples was reported more than 80 years ago as an alternative to the detection of elemental fluorine in spectroscopy [28].

The first document dealing with the improvement of the analytical capabilities of LIBS using molecular emission instead of atomic emission was published by Haisch *et al*. [29] in 1996. In this manuscript, the enhancement of the signal to background ratio for the detection of chlorine in gases was showed by using the emission spectrum of the CuCl D-system instead of the atomic Cl emission line at 837.6 nm. This approach seemed to be banished to oblivion until 2014. However, in the last years several works were published exploring the suitability of this approach for different applications. In 2014 Gaft *et al*. [30] showed the capability of measuring F and Cl by detecting different molecules such as CaF, BaF, MgF, CaCl, SrCl or MgCl.

Table 1 collects the molecular systems in the UV-VIS region of CaF and CaCl [31,32], which are typically used for measuring F and Cl, and **Figure 1a** shows the molecular spectra for CaCl (systems B-X and A-X). Although this work was mainly focused in the molecule formation and detection from a qualitative point of view, higher intensity of the molecular emission in comparison with the atomic one was demonstrated at ambient conditions. In the same year, Alvarez *et al*. [33] described the application of CaF molecular emission (B-X system) for the quantification of fluorite in mining materials with high content of fluorite (in the % range). In a next work [34], the same authors found that in order to carry out quantitative analysis of fluorine by detecting CaF, a molar ratio 20:1 between calcium and fluorine was required. The LOD obtained in this study (about 50 mg g^{-1}) was the lowest detection limit for fluorine in solid samples achieved in LIBS until this moment. **Figure 1b** shows the emission spectrum of CaF molecule (B – X system) recorded for a sample consisting of a Cu matrix containing F and Ca. As can be seen, in absence of Ca and F or in absence of F, the spectra in the region between 520 and 550 nm only shows emission lines corresponding to Cu or Cu and Ca respectively, as well as molecular emission from Ca related species. In 2017, the same authors showed a new methodology to detect F via detection of CaF emission bands in Ca-free samples [35]. In this work the incorporation of Ca to the plasma for molecule formation was proposed by the nebulization of a Ca solution over the sample, simultaneously with the LIBS experiments. This methodology provided limits of detection similar to the ones obtained for Ca containing samples. **Figure 1c** shows a schematic of the experimental set-up to carry out LIBS experiments including nebulization.

The detection of CaF and CaCl molecular bands allowed to assure the presence of F-bearing and Cl-bearing minerals in rock [36]. The data from the ChemCam

instrument on board the Mars Science Laboratory rover Curiosity reported the first analyses of fluorine on Mars in 2015. On the other hand, Vogt *et al*. [37] investigated the use of CaCl and MgCl emission for chlorine quantification in Martian environment. They studied, under simulated Martian conditions, the influence of several parameters such as Ca/Mg and Cl concentrations or the plasma dynamics on the intensities of the emission bands detected. Moreover, the influence of the sample composition was considered to evaluate how the initial bonds of Ca, F and Cl affect the final molecular emission signal, as well as to investigate the competitive process during the molecular formation in the plasma [38]. Additionally, Dietz *et al*. [39] recently demonstrated that the ratio between CaCl and CaOH molecular emission in cements provided lower variations than the CaCl emission alone. It is considered that the molecular emission suffers more fluctuations than the elemental emission, since the molecular formation process depends strongly on the plasma physical conditions.

In 2016 Gaft *et al*. [40] patented a methodology to detect halogens, rare earth elements and boron in samples detecting the molecular emission produced in a plasma generated by double pulse LIBS. This publication described the preferred molecule to be detected depending on the element of interest, for example the dimer formed by Ca and the halogen is appropriate for the halogens (F, Cl, Br and I) although MgCl, SrCl, BaF, or SrF can be also a good selection. On the other hand, the dimer formed with oxygen seems to be the most suitable selection for detecting rare earths and boron. The determination of Br and I was also recently investigated by Gaft *et al*. [41], making use of molecular emission together with double pulse LIBS to increase the detection capabilities. Nevertheless, the presence of CaO might strongly interfere the emission from CaBr and CaI. In the case of samples without oxygen, the analysis in neutral gases atmosphere should be used to avoid the

creation of the interferant species. Furthermore, the use of Ba instead of Ca could be an interesting approach; unfortunately, as Ba is less common than Ca, it could be necessary to add it from an external source.

2.3. Laser induced breakdown spectroscopy molecular isotopic spectrometry (LAMIS)

Isotopic analysis from atomic spectra obtained by optical emission spectroscopy is limited to few spectral emission lines and few elements due to their small isotopic shifts. To resolve the emission lines corresponding to two different isotopes their shift should be higher than the width of the detected emission lines. Although the instrumental broadening of the spectroscopic systems can be an important parameter that prevent the isotope analysis, in the case of LIBS technique, the large Stark broadenings (especially at short times after the laser shot) hamper this type of analysis even for elements and emission lines with the highest isotope shifts. For example, isotopic shift of $_1D^2/_1H^1$ is as large as 0.180 nm for the H_α (656.279 nm) and D_α (656.099 nm) emission lines, but these lines present significant Stark broadening in laser induced plasmas [42].

In order to reduce the Stark broadening as much as possible, and thus to improve the resolution, several approaches could be used. In the work of D'Ulivo *et al*. [43], the delay time was optimized to reduce the Stark broadening on the Balmer alpha emission line of H, and thus to better resolve the two atomic lines coming from the different isotopes. Ratios were then determined via a two-peak Lorentzian deconvolution of the lines. The counterpart of this approach was the fast decay of the emission intensity, limiting the sensitivity. On the other hand, Pietsch *et al*. [44] demonstrated that a combination of reduced pressure, optimized delay time and measurements at appropriate plasma height helps to reduce the Stark and Doppler broadening effects, allowing the isotopic analysis of ^{235}U-^{238}U ionic line at 424.42 nm,

with an isotopic shift of 0.025 nm. In a similar way, Smith *et al*. [45] carried out isotopic analysis of ^{239}Pu-^{240}Pu measuring the atomic emission line at 594.52 nm (isotopic shift of 0.005 nm) using gas batches (He) at reduced pressure and optimized detection conditions.

In the last years, a new approach for isotopic analyses using LIBS has been investigated. It consists on the detection of the emission bands of molecules formed by the isotopes of interest with other species present in the LIBS plasma. The molecular isotopic shifts are larger than the atomic ones; therefore, the discrimination between emission bands of molecules formed by two different isotopes has lower experimental difficulties. The isotopic shifts are due to small differences in the energy levels of two isotopes, which are caused by their different masses as well as slight differences in the Coulombian field generated by the nuclei. In atoms, these corrections can only affect to the energy of the electronic states, being this a small effect. However, in molecules, the different masses of the isotopes mainly affect the vibrational and rotational energy levels, giving as a result larger isotopic shifts. Although the use of molecular spectra to obtain the isotopic ratio of boron at low pressure LIBS was reported by Niki *et al*. [46] in 1998; it has been in the last few years when this approach was expanded by the group of Dr. Russo in the Berkeley Lab (USA) [6,47-50].

Figure 2a shows a comparison between the atomic and molecular isotopic shifts for various elements and diatomic molecules (e.g. oxides and fluorides), showing that the molecular isotopic shift can be orders of magnitude larger than the atomic one. These large isotope shifts permit to resolve the emission from different isotopes without using high resolution spectrographs or reduced pressures in ablation chambers. **Figure 2b** shows the emission bands of the electronic system $A\,^1\Sigma^+ -$

$X\ ^1\Sigma^+$ of SrO. As can be observed, the bandheads of the different isotopes are clearly resolved, so the distinction of the emission of each isotope could be easily performed by comparison of isotopically pure samples containing the element of interest, or by comparing the recorded spectra with simulated ones.

Table 2 collects some examples for which LAMIS was successfully applied. The table shows the isotopes, the molecule formed as well as the electronic system and the emission band detected for the isotopic analysis.

Regarding the quantitative determination of elemental isotopic ratios in a sample, different approaches were investigated using LAMIS. An empirical approach was based on building a multivariate calibration using a partial least square regression (PLSR) model from known reference samples with known isotopic abundance, and the further application of the PLSR model to the unknown sample. The model finds the relationship between the ratios of the bandhead intensities of two isotopes calculated for all the bands used in the calibration and the known isotopic abundance ratios of the samples used for calibration. On the other hand, the isotopic ratio of a particular element in a given unknown sample could be obtained by comparing the recorded molecular spectrum with a simulated one, which must contain the most important isotopic contribution, and then fitting the simulated spectrum to the experimental one, considering the isotope ratio as fitting parameter [51].

Although data treatment processes might seem more complex and laborious than those typical used in elemental LIBS analysis (e.g., the use of integrated areas of elemental lines), LAMIS offers better results in isotopic analysis than those obtained by traditional LIBS analysis, even when the isotopic shifts are big enough to allow elemental isotopic analysis. In this context, the identification of H-D or ^{235}U-^{238}U seems to point that the use of LAMIS, or even the combination of molecular and

atomic information (LAMIS-LIBS) improves the accuracy of the isotopic analysis of the elements [42,48].

Summarizing, LAMIS improves the range of applicability of LIBS technique for isotopic analysis thanks to the larger molecular isotopic shifts. The main requirement is that the element of interest must form a molecule (typically with O), which must be detectable by LIBS. It is noted that the number of isotopes investigated by this technique is increasing in the last years. Nevertheless, LAMIS needs further development to improve the analytical capabilities of the technique, mainly to increase its sensitivity without losing some of the most important LIBS advantages, such us minimum sample preparation or the capability to carry out stand-off measurements [52]. Also, the presence of atomic emission interferences from other compounds found in the sample could reduce the capabilities to obtain the proper isotopic ratios.

In any case, the possibility to identify different isotopes at ambient conditions can be used to better understand some of the physical mechanisms that govern the laser-induced plasma, such as the different molecular processes, using isotopically enriched samples [53,54].

3. Molecular analysis using optical atomic sources: Molecular absorption spectrometry

3.1. Introduction

The field of atomic absorption has experienced a sort of revolution with the arrival of high-resolution continuum source atomic absorption spectrometers (HR CS AAS), using both flame (F) or graphite furnace atomizers (GF) [55]. The idea of using continuum sources instead of line sources for AAS is certainly not new, as it can be traced back

practically to the origin of the technique, and different devices were designed based on such concept [56]. It has to be kept in mind, as discussed in the introduction, that achieving sufficient resolution is always paramount when designing an instrument based on a continuum source, because otherwise it would be impossible to properly separate the atomic signal from the background.

The work carried out by Becker-Ross *et al*. [57–59] finally proved successful providing the basis for a commercially available instrument, which comprises the following major components: (i) a high-pressure xenon short-arc lamp, capable of providing high intensity in the UV-VIS region; (ii) a double monochromator, which consists of a prism with an echelle grating afterwards; and (iii) a linear CCD array, as detector.

The advantages of such instrument are numerous and have been covered in several dedicated reviews [60-62]. In our view, it is key to mention that such type of instrument adds a new dimension (wavelength) to the classic bidimensional (time and absorption) AAS. This aspect is critical because it enables the analyst to observe not only the expected signal but also everything surrounding it, which can ultimately affect its measurement [2,3]. Thus, such type of instrument provides better tools for the detection and correction of spectral interferences, which facilitates the direct analysis of solid samples and complex liquids, as discussed in detail elsewhere [63].

In the context of the current review, what is remarkable is that the resolution attainable by this device permits to monitor and quantify not only atomic transitions, but also molecular ones. Even at the typical temperatures found in a flame or a graphite furnace, some diatomic molecules persist in gas phase and many are capable of absorbing radiation in the UV-VIS region. In short, what is monitored with the level of resolution (picometer level) attainable in an HR CS AAS device are the vibrational

and/or rotational transitions superimposed to the molecular electronic transitions, which fall into this spectral region. For a more detailed explanation of the optical processes occurring the reader is referred to the review of Welz *et al*. [4]

3.2. Advantages of monitoring highly resolved molecular spectra

3.2.1. Background correction, non-metals and challenging metals

Possessing the capability of monitoring highly resolved molecular spectra opens up several possibilities. First, it has to be stated that when the goal is to monitor atomic absorption, this type of molecular absorption represents a potential interference. A structured and rapidly changing background that is very difficult to correct for when using line sources, if it overlaps with the analyte signal. In the case of HR CS AAS this is not such a serious problem, as long as the source for this “background” can be properly identified, such that a suitable reference spectrum (containing only the interfering molecule) can be obtained. This reference spectrum can be proportionally subtracted from the original signal by means of least-squares background correction (LSBC), and the result should contain only the atomic absorption signal of the analyte. Several examples of the successful application of this strategy had been reported in the literature since the first one, published by Becker-Ross *et al*. [59], which demonstrated the potential of this approach to determine challenging elements such as As and Se. Even in cases where the interference is caused by two molecules, it is still possible to correct for them sequentially and finally obtain only the target atomic signal [59,64]. This strategy is particularly important to determine elements that show their main lines around 250 nm or below (e.g., metalloids), as several molecular species (e.g., based on the presence of N, P, S, or Si, to name a few ubiquitous elements) possess bands in this region of the UV.

A second and critical advantage of this possibility to monitor molecular lines is that it enables the determination of elements that are either very difficult or almost impossible to determine using atomic lines. As stated in the introduction, we are referring to non-metals such as the halogens, nitrogen, phosphor or sulfur. Selected examples of such determinations are shown in **Table 3**. This table cannot be comprehensive, as neither the purpose nor the expected length of the current article enables such approach. Instead, the reader is referred to the review of Welz *et al*. already mentioned above for early works [4], to reviews [65] and [66], and finally to review [5] for the most updated information (last five years). In the particular case of sulfur determination, there is another review available [67].

The basic idea of these works is always the formation of a diatomic molecule containing the element of interest [68]. The formation of such molecule can be spontaneous, without the need to add any reagent. For instance, let's suppose that the goal is to determine S. Such possibility is very challenging *via* atomic absorption because S main atomic lines are not located in the UV-VIS region. However, as in both a graphite furnace and in an acetylene flame there is plenty of carbon available, forming the CS molecule in gaseous phase in the presence of S compounds is simple. Thus, under optimized conditions, the amount of sulfur in a sample can be quantified *via* the measurement of CS transitions [69]. An example of a 3D CS absorption spectrum as obtained with HR CS GF MAS is shown in **Figure 3a**. The figure shows the $\Delta v=0$ vibrational sequence of the electronic transition $X\ ^1\Sigma^+ \rightarrow A\ ^1\Pi$ [68]. This spectrum shows many sharp rotational lines with a width of a few picometers (similar to the width typically observed for atomic lines), that can be measured and used for quantification due to the high-resolution available. It is important to remark that, as can be noticed in **Figure 3**, the commercial instrumentation currently available to

perform HR CS MAS is very limited in terms of the spectral window that can be simultaneously monitored [70–72]. The instrumentation actually offers only values from 200 detector pixels. This fact, combined with the high resolution, approx. 1 pm in the UV region, means that only 0.2-0.3 nm are simultaneously measured in such region. This value increases in the visible region up to almost 1 nm, at the cost of subsequently decreasing the resolution proportionally (even though the latter is not a relevant problem in practice, as the potential for overlaps in this region is lower). Thus, only a small portion of the complete molecular spectrum can be actually measured at a given time. That may change in the future, as it is technically possible to improve this aspect substantially without losing resolution, and the use of a prototype with drastically improved capabilities has already been reported by Geisler *et al*. [73]. Also, Labusov *et al*. have presented another prototype with a much wider spectral window (190-780 nm), although with a resolution of only 10 to 30 pm [74]. Therefore, there is certainly potential for a commercial instrument capable of measuring both atomic and molecular absorption in the whole UV-VIS region simultaneously, which will expand the multielemental capabilities of the technique enormously. However, this limitation is an important aspect to keep in mind for the time being.

In many situations, it is not possible to produce the target molecule spontaneously. Thus, it is necessary to add a substance in sufficient excess to form such molecule (e.g., a Ca salt to form CaCl, an Al salt to form AlF, a Ba salt to form BaI, etc.), which is often referred to as molecule forming agent. Most of the examples shown in **Table 3** belong to this category. This target molecule needs to be stable enough at the high temperatures of a graphite furnace or a flame and, also, absorb radiation in the UV-VIS region with sufficient sensitivity. **Table 3** shows several examples of typical molecules

used, with information on the characteristic mass and limit of detection that can be attained, both *via* flame and graphite furnace. Obviously, HR CS GF MAS is more sensitive, but still the sensitivity obtained is two or three orders of magnitude lower in comparison with what can be typically observed for metals using HR CS GF AAS (characteristic mass at the 1-10 pg level, in the best cases). F is an exception, as it is an element that can be determined with great sensitivity *via* HR CS GF MAS, while it is very complex to determine it using other atomic techniques [75]. Therefore, it is one of the non-metals most often determined using HR CS MAS [5].

The spectrum obtained *via* HR CS MAS is not always as rich in lines as the one shown for the CS molecule; sometimes only a broad band is observed (this is typically the case when Al is added as the molecule forming agent, to produce, for instance AlBr, AlCl or AlF) [76]. However, most often several transitions are simultaneously monitored. Another example of this situation is shown in **Figure 3b** (CaBr electronic transition $X^2\Sigma^+ \rightarrow A^2\Pi$) [77].

It can be stressed that it is always beneficial to have several lines to choose from. There is always the possibility to combine the signal of several transitions to improve the LOD a bit [78]. Alternatively, this may provide a simple way to expand the working range, as the transition that is more suitable for the particular analyte content of each sample can be selected, even off-line after the measurements are done [63].

Moreover, the simultaneous monitoring of several transitions has been shown to enable a new calibration approach called multi-energy calibration, which uses these several lines instead of needing the preparation of several aqueous standards for calibration. Such method requires measuring only two solutions: one (S1) prepared by mixing a standard of known concentration with the sample (1:1, v/v), and another one (S2) that mixes a blank solution with the sample (also, 1:1, v/v). Then, the absorbances

obtained for all the lines monitored for S1 and S2 are plotted and linear regression is performed. It is beyond this review to describe how the sample concentration is derived from the equation obtained, but with this approach Cl (as CaCl), N (as NO), P (as PO) and S (as CS) were determined in several samples: Cl in milk powder, after preparing water suspensions; N and P in liquid fertilizers, after dilution in water; and N and S in commercial salts, after their dissolution in water [79].

Finally, while the vast majority of applications of HR CS MAS have focused on the determination of non-metals for the reason explained before, there are situations where the determination of metals could also be advantageous. For instance, use of AlF transitions instead of Al atomic lines may serve to overcome some matrix and spectral overlaps for the determination of Al in blood [76]. In such case, a fluorinating agent is added as molecule forming agent. Also for Al, use of the AlH line instead of the atomic line enabled the simultaneous determination of Al, Cr and Fe in soil samples, as rotational transitions of AlH (spontaneously formed in the presence of a sufficient amount of Al) can be measured together with atomic lines of Cr and Fe [80], while that is not the case if only atomic lines are used due to the limitations in the spectral window that is simultaneously recorded with current HR CS AAS instruments, as already discussed at the beginning of this section.

Another case concerning Si determination in a flame has been reported recently. While it is possible to produce Si atoms in a flame, this typically requires using N_2O-C_2H_2, which represents a hazard. Instead, by monitoring SiO it is possible to achieve LODs below the 1 mg L^{-1} level for the determination of organic Si, with the usual and less dangerous air-acetylene flame. Thus, the analyst can decide: if the best sensitivity is required, the production of silicon atoms in a N_2O-C_2H_2 flame still is the best option

(about 10 times better detectability), but if not, the measurement of SiO is an interesting alternative [81].

3.2.2. Isotopic analysis

The final important advantage that can be achieved when using molecular and not atomic absorption is the better access to isotopic information.

While in principle it is possible to obtain isotopic information using atomic absorption signals too, as atomic transitions originating from different isotopes of the same element do not absorb radiation exactly at the same wavelength, in practice this approach shows great limitations. The reasons are the same discussed before (section 2.3.) for LIBS: the isotopic shifts for atomic transitions are extremely small, and several effects (e.g., collisional broadening, Doppler and Stark effects) produce the broadening of their peaks, further hampering the possibility of observing separate isotopic lines, even if instrumentation with very high resolution (1 pm) is available. Thus, this approach is limited to a few elements that show comparatively large atomic shifts (e.g., light elements such as B) [82].

However, it is also well-known that molecules are prone to show much larger isotopic shifts, as also discussed in section 2.3. when introducing LAMIS [6]. The same basic idea applies herein for absorption techniques. If instead of monitoring atomic absorption lines, the spectrum of diatomic molecules is targeted, then a significant isotopic shift can be appreciated, potentially leading to the separate quantification of the different isotopes of an element.

This idea has been explored only recently, so very few papers have been published on this topic. The first one aimed at the isotopic analysis of Cl, *via* the

formation of AlCl. Since Al is monoisotopic, the resulting shift would be due to differences between ^{35}Cl and ^{37}Cl only [83].

Figure 4 shows the signals obtained for the AlCl $X^1\Sigma^+ \rightarrow A^1\Pi$ electronic transition (vibrational transition $\nu',\nu''=4,4$, where ν' is the vibrational quantum number of the upper level, and ν'' that of the lower level involved in the transition), obtained under optimized conditions *via* HR CS GF MAS. Two peaks (one for $Al^{37}Cl$ and one for $Al^{35}Cl$) that are sufficiently separated away (approximately 24.3 pm) can be appreciated, and their respective signals seem to be in good agreement with the expected values, because the solution was prepared to provide a $^{35}Cl/^{37}Cl$ value of 1. It has to be indicated that the magnitude of the shift observed for this electronic transition depends on the vibrational levels and, unfortunately, the most populated ones that lead to higher sensitivity ($\nu',\nu''=0,0$) practically show no shift. The shift increases for transitions between higher vibrational levels, being sufficiently high to observe two peaks with minimal overlap from $\nu',\nu''=3,3$ (15.6 pm) on. Thus, a compromise has to be reached between the sensitivity and the magnitude of the shift, depending on the expected analyte levels.

In any case, it is clear that the magnitude of the shifts (which can be predicted using the expression proposed by Herzberg [84]) is large enough to enable HR CS GF MAS monitoring. In fact, it was demonstrated in the work that it is possible to perform the isotopic analysis of Cl in solutions of 20 mg L^{-1} with precision values of approximately 2% RSD (using the $\nu',\nu''=3,3$, with $Al^{35}Cl$ appearing at 262.238 nm). Such values are not low enough to appreciate natural variations in the isotopic composition of Cl, but they suffice for tracer experiments or for performing isotope dilution (ID). In this regard, the use of ID for calibration enabled accurate results for different types of water samples to be obtained, even in the presence of interferences

originating from the presence of other substances that would otherwise affect the signal (e.g., the presence of high levels of Ca shows a clear effect on the AlCl signal).

The next work on this topic investigated the use of HR CS GF MAS for isotopic analysis of Br, *via* the CaBr molecule, which was selected after investigating other target molecules, such as AlBr or BaBr. Several CaBr lines that could be simultaneously monitored were found to respond selectively to the presence of $Ca^{79}Br$ or $Ca^{81}Br$, respectively. Using a Br solution of 10 mg L^{-1}, a precision of 2.6% was reported. This is again hardly sufficient for investigating Br natural isotopic variations. However, the potential of ID was highlighted again, as it was proven that with such calibration approach it became possible to determine Br directly in solid samples, circumventing the occurrence of interferences of chemical origin (presence of very high levels of Cl, decreasing the formation rate of CaBr since the formation of the most stable CaCl molecule will be favored in such conditions [85]).

Another work reporting on isotopic analysis using HR CS GF MAS was published by Abad *et al.* [86], investigating B. However, instead of targeting B atomic lines, it was the BH molecule the one that was formed and measured. Two different spectral windows were monitored, one in the proximity of 433.1 nm and one around 437.1 nm. The method developed cannot be considered as sensitive, as it requires the presence of at least 1 g L^{-1} of the analyte. It has to be reminded again that the sensitivity of HR CS MAS can hardly compete with that of HR CS AAS, much less when looking at transitions with larger shifts. However, a remarkable precision was achieved. A library of BH molecular spectra was built after the measurement of solutions with different ^{11}B fractions, enabling analysis *via* partial least squared regression of various isotopic reference materials and sample solutions, and

reporting uncertainties (k=2) between 0.013 and 0.05% for the 437.1 nm region. This level of precision should permit investigating B natural isotopic variations.

Finally, a recent article by Zanatta *et al.* explored the use of HR CS GF MAS for the isotope determination of a metal, Ca in this case [87]. The idea was to add F as molecule forming element and monitor CaF, because the difference in wavelength between ^{40}CaF (maximum at 628.534 nm) and ^{44}CaF (maximum at 628.191 nm) absorption signals was found to be rather large: 337.8 pm. Instead of trying to calculate natural isotope ratios with high precision, which is difficult due to the high differences in abundance between ^{40}Ca and the other Ca isotopes, the work demonstrated that it is possible to determine simultaneously ^{40}Ca and ^{44}Ca using a specific calibration curve for each Ca isotope. Satisfactory recoveries for the determination of ^{40}Ca and ^{44}Ca in three urine samples spiked with different amounts of both isotopes was reported, with LODs varying between 1 and 2 mg L^{-1}, depending of the pH selected. It has to be noted, however, that for analysis of these real samples, the method also requires Ca separation from the matrix by precipitation with ammonium oxalate, to avoid the chemical interferences derived from the presence of a high amount of Cl in urine, thus favoring the formation of CaCl instead of CaF. Chemical interferences are a recurrent problem when attempting HR CS GF MAS, as will be discussed below.

3.3. Challenges associated with the monitoring of molecular spectra

Besides the mostly positive aspects discussed before, it is important to also discuss the most relevant issues that still need to be addressed, as well as those aspects that need to be carefully optimized during method development. Many of them have already been hinted at in the sections before, even if very briefly.

For successful monitoring of molecular spectra using HR CS MAS, it is necessary to form a molecule that is stable enough and that possesses transitions that can provide sufficient sensitivity. As a reference, Welz *et al*. advice the use of diatomic molecules with a bond strength of at least 500 kJ mol $^{-1}$ [4]. Use of other diatomic molecules can be targeted on occasions, but they are more prone to suffer from interferences caused by the presence of other chemical compounds. If we look at the halogens, for instance, F tend to bond with higher strength with most elements than Cl, Cl bonds stronger than Br, and Br stronger than I. Thus, it is much easier to find suitable molecules and conditions to determine F and Cl, than to determine Br, and it is actually difficult to determine I, because even though there are some molecules than can be measured (such as BaI, CaI, InI or SrI) [88,89], if the sample contains higher amounts of other non-metallic species (and Cl, for instance, is found at high levels in many biological samples, where determination of I is of great interest), formation of alternative species (such as BaCl, CaCl, InCl or SrCl) will always be favored, thus resulting in a loss of sensitivity for I determination, and in serious difficulties to calibrate. As discussed before, use of isotope dilution is one of the solutions that can help to overcome this problem, as long as the loss of sensitivity is not complete [85].

In addition, if a spectrum with many transitions is going to be produced, it is necessary to check that there are not spectral overlaps affecting the lines that will be finally selected for quantification. In this regard, selecting the right diatomic molecule can help in minimizing both matrix and/or spectral effects. For instance, CaX (where X is a halogen) molecules show their main lines in the visible region of the spectra, which is typically less affected by spectral interferences than the UV region. Moreover, many biological samples already contain very high levels of Ca, which can result in an interference if a molecule with a different metal is targeted. So, in many cases, it makes

sense to use Ca as molecule forming agent instead of competing against this metal. Finally, Ca often stabilizes also halogens, so it can act as both chemical modifier and molecule forming agent [90]. All these reasons can explain the increasing popularity of the use of Ca as molecule forming agent for the determination of halogens. Its use also results in some disadvantage, though, as Ca interacts with graphite, deteriorating the tube and the platforms faster.

Use of suitable chemical modifiers is always important when using GF AAS. However, in the case of HR CS GF MAS it may result even more critical to try to minimize these interferences of chemical origin mentioned above. It has to be reminded that the atomization procedure in AAS is relatively simple, as it ultimately relies on the temperature to finally produce free atoms of the analyte in the gas phase. In the case of MAS, it cannot always be guaranteed that the target molecule will be formed in a reproducible manner, unless the chemistry is properly controlled. Moreover, many non-metals form very volatile species, and thus it is important to prevent losses during pyrolysis. Also, the analytical response obtained for different species containing the target element may be different. This aspect needs to be prevented by careful selection of the chemical modifier and temperature program [63,91], but in some favorable cases it may allow for the development of speciation methods. For instance, it has been reported that the rate of NO production from nitrate and nitrite is very different [92], potentially enabling the separate determination of both species, although most speciation approaches based on HR CS MAS require different sample preparation or separation strategies [93–95].

4. Monitoring of molecular species in inductively coupled plasma – mass spectrometry (ICP-MS)

4.1. Introduction and theoretical background

In the field of atomic spectrometry, ICP-MS is the most powerful technique for ultra-trace elemental and isotopic analysis for a large variety of sample types. When compared to other analytical techniques, ICP-MS offers several advantages, such as the low limits of detection attainable (down to the ng L^{-1} level), wide linear dynamic range (up to 10 orders of magnitude), high sample throughput and multi-element capabilities. Furthermore, ICP-MS can easily be combined with alternative sample introduction systems, such as laser ablation (LA) for the direct analysis of solid samples, and chromatographic separation techniques for speciation analysis. A relatively new trend in ICP-MS is related with the possibility of obtaining temporally and spatially resolved information, allowing for the characterization of nanoparticles and individual cells and for high-resolution imaging of the distribution of elements in 2 or 3 dimensions. A major disadvantage of ICP-MS is the relatively high capital and running cost. However, the most important drawback of this technique is the occurrence of spectral interferences. Since the commercial introduction of ICP-MS in 1983, different strategies have been developed to avoid spectral overlap in a more efficient and straightforward way. A review of those methods is beyond the scope of this review; for more information on the different approaches developed over the years, various papers devoted to this topic can be consulted [96–100]. The introduction of collision/reaction cell (CRC) technology in 1996 was a significant breakthrough in the field of ICP-MS and a step further towards the monitoring of molecular ions using an *a priori* atomic technique [101,102]. Before, polyatomic ions were only monitored in an attempt to quantify an element's content for which the M^+ signal intensity (*i*) exceeded the upper limit of the working range of the electron multiplier operated in pulse-counting mode, or (*ii*) was affected by the occurrence of spectral overlap that could be addressed by using a mathematical equation for

correction [103]. The correction for the contribution of $^{40}Ar^{35}Cl^{+}$ to the total signal intensity at a mass-to-charge ratio of 75 based on the measurement of $^{40}Ar^{37}Cl^{+}$, thus enabling accurate ^{75}As determination can serve as an example of the latter approach. The introduction of CRC technology in quadrupole-based (Q) ICP-MS instrumentation, intended for avoiding or at least minimizing the occurrence of spectral interferences changed this situation [104]. One way of accomplishing interference-free conditions is by using a non-reactive collision gas to selectively slow down polyatomic interfering ions, enabling their removal from the ion beam by means of kinetic energy discrimination [105]. A second approach that can be used in a CRC, which is more relevant in the context of this review paper, is chemical resolution. By using this approach, the cell is pressurized with a reaction gas that can react either with the target ion or with the interfering ion(s), thus creating interference-free conditions [106]. In the on-mass approach, the interfering ions are neutralized, broken down into the constituting atoms/atomic ions or converted into a reaction product ion, with another mass-to-charge (m/z) ratio, thus enabling quantification of the target element on the basis of the signal of its atomic ion. Optimum performance in an on-mass approach requires the interfering ion(s) to be removed completely. In the mass-shift approach, on the contrary, it is the target atomic ion that is converted into a molecular reaction product ion with a different m/z ratio. An important advantage of this approach is that this conversion does not need to proceed quantitatively as quantification in ICP-MS always relies on comparison of the signal intensities for samples and standard(s). However, obtaining sufficient insight into the chemical processes occurring within a CRC is not always self-evident.

The first studies reporting on the use of ion-molecule chemistry within a pressurized multipole cell already date from 1989. Rowan and Houk demonstrated

that the use of reactions between plasma-generated ions and the molecules of different gases could be an effective approach to avoid spectral overlap in ICP-QMS [107]. In this context, one of the main challenges is the selection of an appropriate gas and the reaction exploited to achieve interference-free conditions. For this purpose, gas-phase ion-molecule processes have been extensively studied and documented using different techniques (*e.g.*, ICP – selected-ion flow tube (SIFT) – MS) [108,109]. However, the conditions in a pressurized multipole cell of an ICP-QMS instrument are such that the reactivity of a given ion towards a selected reaction gas is not always identical to that observed using other techniques. In other words, the selection of a reaction gas for the formation of a new molecular reaction product ion cannot only be based on the currently existing databases (although they can be used as starting point). These differences can most likely be explained by the different conditions under which these reactions proceed, as typically the studies conducted to evaluate the reactivity have been carried out under thermal conditions. In absence of an external source of energy, only exothermic reactions can occur. However, in an ICP-CRC-QMS instrument, these requirements are not always fulfilled. In a CRC, the particles (*i.e.* ions and/or gas molecules) do not have a Maxwell-Boltzmann energy distribution with the same temperature in all degrees of freedom. This is related with the continuous introduction of gas and with the energy of the ions in the beam extracted from the plasma. Therefore, in a CRC, thermal conditions are not obtained [102,110].

As a result, finding a selective ion-molecule process to avoid spectral overlap in ICP-CRC-QMS still remains a challenging task. The reaction selected needs to be thermodynamically and kinetically favorable. The difference in Gibbs free energy accompanying the process (ΔG) determines whether a reaction is thermodynamically

allowed or not, but whether a given reaction is suitable for the analytical purpose intended is rather governed by its reaction rate (kinetics). However, even such a general statement has to be handled with care, as endothermic reactions can also proceed in CRC systems under specific non-thermal circumstances, as occurring at very high concentrations of the reactants and/or when additional sources of energy (*e.g.*, owing to collisions) play a role [99]. Thus, the use of ion-molecule processes occurring within a CRC for overcoming spectral overlap has to be experimentally studied in detail before chemical resolution can be effectively applied in a real-life analytical context.

4.2 Single quadrupole vs tandem ICP-MS instrumentation

Widespread use of mass-shift approaches to avoid spectral overlap has typically been hindered by the lack of control over the ion-molecule processes occurring within the CRC. As a result, for a long while, reactions between the gas selected and the interfering ions (on-mass approach) have typically been preferred over the formation of new molecular reaction product ions (mass-shift approach), despite the fact that for the on-mass approach, 100% reaction efficiency is required to completely remove the interfering ions. In contrast, as discussed before, partial conversion of the target ion into a reaction product ion suffices for mass-shift approaches, as long as this reaction efficiency is constant over time and there is no other atomic ion hindering monitoring of the reaction product ion at the new m/z ratio. Obviously, some other issues need to be addressed (see next section), such as the selection of a suitable reaction gas, optimization of the gas flow rate (gas pressure in the CRC), identification of the best reaction product ion to monitor and the occurrence of unwanted reactions with matrix ions, potentially hampering interference-free

monitoring of the target molecular ion. In 2012, the first commercially available tandem ICP-MS instrument (ICP-MS/MS) was introduced onto the market by Agilent Technologies. Such type of instrument is often colloquially referred to as “triple quadrupole”, a term that is not entirely correct. Since then, the number of ICP-MS works reporting on the use of molecular ions for ultra-trace elemental, speciation and isotopic analysis has grown exponentially, leading to the introduction of an updated version of such instrument in 2016, while also ThermoFisher Scientific launched its first tandem ICP-MS instrument in 2017. Briefly, in the tandem ICP-MS design, an additional quadrupole is located in front of the CRC (**Figure 5** shows the benefits of the MS/MS configuration for the interference-free determination of Cl; for this specific example, the readers are referred to section 4.3.2). This set-up provides much better control over the reactions occurring within the CRC and offers novel tools to systematically study these processes, thus facilitating the selection of optimum conditions and the use of molecular reaction product ions in trace element analysis [111,112]. A first crucial benefit is that the atomic ion potentially occurring at the m/z ratio of the reaction product ion is removed by the first quadrupole. Mass selection by the first quadrupole also largely prevents the formation of unwanted reaction product ions potentially overlapping with the target molecular ion as a result of the rejection of all m/z ratios different from that of the target analyte. This also provides a better control over the ion-molecule processes occurring within the CRC, *e.g.*, selection of the best suited reaction product ion (see examples of the use of these features below), while powerful tools are provided for facilitated method development. It needs to be stressed that the monitoring of molecular reaction product ions is not restricted to tandem ICP-MS instrumentation, but the latter instrumentation undoubtedly extends the application range of this approach and facilitates its use, thus justifying

focusing on this specific technology when discussing about the monitoring of molecular ions using ICP-QMS.

4.3. Molecular ion monitoring using ICP-MS(/MS)

4.3.1. Reaction gas(es) and molecular ion(s) selection

Before an ICP-MS mass-shift approach can be used for analytical purposes, the best suited molecular ion must be selected. Therefore, the first step of this method development is the selection of a gas that selectively and efficiently reacts with the analyte ion of interest and the identification of the ion-molecule processes occurring within the CRC. In this context, different reaction gases, including, *e.g.*, H_2, O_2, N_2O, NH_3, CH_3F, SF_6 (non-exclusive list) have been explored [113]. Depending on the gas selected and its reactivity, the reaction product ions thus obtained can be more or less complex (contain more or less constituting atoms), thus leading to a wide variety of molecular reaction product ions, ranging from diatomic to cluster molecules. Oxygen is an example of a gas typically forming relatively simple molecular ions, *i.e.* oxides and/or dioxides (MO^+ and MO_2^+) [114,115]. In this case, the m/z ratio of the newly created ionic species can be identified easily, as the m/z ratio of the analyte of interest with the addition of one or two oxygen atoms, *i.e.*, +16 or +32 amu, respectively. However, in the case of highly reactive gases, such as ammonia, many different NH_3-based cluster ions ($M(NH)_x(NH_2)_y(NH_3)_z^+$) can be formed, distributed across the mass spectrum [116]. As a result, the selection of the best suited reaction product(s), free from spectral interference and providing the highest signal-to-background ratio, is not always self-evident.

ICP-MS/MS instrumentation fortunately provides several tools to facilitate this task, the most powerful one being product ion scanning (PIS). For PIS, the first quadrupole is fixed at a specific m/z ratio (typically that of the target analyte), the cell is pressurized with the reaction gas at a given flow rate, and the second quadrupole scans the entire mass spectrum (2 – 260 amu). In this way, an overview of the reaction product ions formed under such conditions is displayed by plotting their signal intensities (y-axis) *versus* their mass-to-charge ratio (x-axis). This approach can then be repeated at different gas flow rates, thus providing an additional dimension to study the sometimes- complex reactions taking place in a CRC system. **Figure 6** shows an example of product ion scanning to identify the best suited titanium-based reaction product ions using O_2 (a) and NH_3 (b) reaction gases; the readers are referred to section 4.3.2 for more information about this specific work.

As indicated above, chemical resolution is not restricted to MS/MS instrumentation; interference-free conditions can also be obtained in single-quadrupole (SQ) ICP-MS using this strategy. However, the ion-molecule processes proceeding in the CRC of an MS/MS instrument might be different from those occurring in the CRC of a single-quadrupole ICP-MS unit. Differences can occur as a result of the introduction of large amounts of plasma-based and matrix ions entering the CRC in the absence of a first quadrupole mass filter, while in MS/MS, the first quadrupole removes all ions with a m/z ratio different from that of the target analyte. The presence of large amounts of these ions in the cell in single-quadrupole ICP-MS may change the ion-molecule chemistry, while also undesired side reactions can occur, leading to unwanted reaction product ions with the same m/z ratio as that of the reaction product ion(s) selected for the elements of interest. It needs to be noted, though, that a quadrupole-based CRC (but not those based on an hexapole or

octopole setup) can also be used as a bandpass mass filter to avoid secondary chemistry [116,117]. Amplitude and frequency of the AC component and amplitude of the DC component applied between pole pairs (the Mathieu parameters q and a, respectively) allow removal of all ions outside of a defined mass window [118]. Although at lower resolution than with MS/MS, defining a mass bandpass with a quadrupole-based CRC permits some secondary reactions to be avoided by using this bandpass mode, thus improving the control over the ion-molecule chemistry occurring within the CRC also in SQ-ICP-MS instrumentation [119,120].

4.3.2. Illustrative examples

Over the years, the monitoring of molecular reaction product ions in ICP-CRC-QMS instrumentation has grown very rapidly, as this can be seen as an effective approach to avoid spectral overlap. This situation is especially true for elements that are strongly affected by the occurrence of interferences from plasma-based and matrix ions in the low mass range (≤80 amu), rare earth elements (REEs) suffering from spectral interference caused by MO^+ ions and/or platinum group elements (PGEs). An overview of illustrative examples of molecular ion monitoring in ICP-MS is provided in **Table 5**.

In this context, phosphorus and sulfur can be considered key elements, both before and after the introduction of tandem ICP-MS. The typical approach consists of oxidizing P^+ (31 amu) and S^+ (32, 33 and 34 amu) atomic ions into PO^+ (47 amu) and SO^+ (48, 49 and 50 amu, respectively) reaction product ions. This approach was already used by Bandura *et al*. using an SQ-ICP-MS instrument equipped with a quadrupole-based CRC for the detection of P and S at ultra-trace concentration levels (<μg L^{-1}) to quantify the degree of phosphorylation of proteins [121]. This

method relies on the lack of reactivity between the most important originally interfering polyatomic ions (*e.g.*, NO^+ and O_2^+) and O_2 gas, as these reactions are endothermic and should not proceed under thermal conditions. However, as indicated in section 4.1, theoretically disallowed reactions can sometimes still occur under the specific circumstances within a CRC system. In addition, an SQ-MS system does not prevent overlap between the newly created reaction product ion(s) (*e.g.*, $^{32}S^{16}O^+$) and concomitant matrix ions with the same nominal mass (*e.g.*, Ca and Ti^+ at 48 amu), unless the new interferences would also be quantitatively (*i.e.* with an efficiency of 100%) mass-shifted towards a higher mass by means of the formation of the corresponding oxide ions (CaO^+ and TiO^+, respectively). Thus, the use of this type of approaches in SQ-MS systems is often prone to interference at the m/z ratio of the newly formed analyte reaction product ion and from unwanted reaction product ions formed upon reaction between concomitant matrix elements and the reaction gas selected, thus reducing the control over the ion-molecule chemistry occurring within the CRC. For other S isotopes, such as ^{34}S, the overlap with the signal from $^{38}Ar^{12}C^+$, and even with signals from other S-based molecular ions, such as $^{33}S^{17}O^+$ or $^{32}S^{18}O^+$, jeopardize an accurate determination based on the SO^+ ion.

Such limitations were overcome by the introduction of MS/MS instrumentation, as the first quadrupole filters out all masses different from that of the target ion (1 amu window bandpass mass filter), thus improving the control over the reactions proceeding in the cell. It is therefore worth mentioning that the first two publications based on the use of ICP-MS/MS reported on (*i*) the interference-free determination of P and S for absolute quantitative proteomics and phosphoproteomics and on (*ii*) the determination of S in organic matrices using isotope dilution for quantification, in that

order [122,123]. In the latter case, it is important to stress that the use of the MS/MS mode also preserves the natural isotopic pattern of S, thus allowing the use of isotope dilution as a calibration approach and opening additional possibilities for isotopic analysis based on the signals of reaction product ions of the target element's isotopes. In fact, the possibility of preserving the isotopic pattern of the elements when monitoring them as reaction product ions is a key advantage of MS/MS over SQ-MS instrumentation. After these works, a plethora of research papers relying on this method for interference-free determination of P and S were published in the scientific literature, describing their use in analytical contexts as diverse as analysis of fuels [124], speciation using the hyphenation of gas chromatography (GC) or high-performance liquid chromatography (HPLC) to ICP-MS/MS for the analysis of pesticides and biological samples [125,126], respectively, laser ablation bioimaging of tissue sections for cancer research [127], or analysis of individual cells using ICP-MS in fast single-event mode [128].

Next to P and S, chlorine (Cl) is another element with low mass (35 and 37 amu) that suffers from spectral overlap and the determination of which using a mass-shift approach is of particular interest. Based on the successful results previously reported for both S and P, monitoring the ClO^+ molecular ions was expected to be the best suited approach. However, it was found that the reaction efficiency between Cl^+ and O_2 is relatively low, and thus, the use of H_2 as reaction gas is typically preferred over that of O_2 for interference-free determination of Cl. Hydrogen has also been widely used (often mixed with He) as reaction gas to remove spectral interferences based on the reactions between H_2 and plasma-based and matrix ions [129]. As an example, $^{28}Si^+$ can be separated from $^{12}C^{16}O^+$ and $^{28}N_2^+$ by converting these polyatomic interfering ions into $^{12}C^{16}O^1H^+$ and $^{28}N_2{}^1H^+$, respectively. However, like

O_2, H_2 can also react with the target ions to create relatively simple molecular ions (MH^+ or MH_2^+). This type of reaction has been used for the determination of $^{35/37}Cl^+$ based on the formation of the molecular ion $^{35/37}ClH_2^+$ (+2 amu). This example clearly illustrates the differences between SQ-MS and MS/MS, as the newly created $^{35}ClH_2^+$ molecular ion would normally overlap with the other Cl isotope (37 amu) in SQ-ICP-MS. In MS/MS however, complete removal of $^{37}Cl^+$ by means of the first quadrupole mass filter in MS/MS mode solves this problem, as demonstrated in various works dealing with the determination of Cl in environmentally and clinically relevant samples [130,131].

Frequently, two or more gases, and thus different reaction product ions, could *a priori* be suitable for overcoming spectral overlap. In such a situation, the molecular ion finally selected should be the one providing the highest sensitivity under interference-free conditions. Sometimes, a compromise between sensitivity and selectivity has to be accepted. As indicated above, H_2 and O_2 reaction gases lead to simple reaction product ions, while other highly reactive gases, such as CH_3F or NH_3, typically result in the formation of more complex cluster ions, distributed more widely across the mass spectrum. As a result, for approximately the same reaction efficiency between the target ion and the reaction gas, those gases giving rise to simple molecular ions (*e.g.*, MO^+) generally provide higher sensitivity and lower selectivity, while the formation of many cluster ions (*e.g.*, $M(NH)_x(NH_2)_y(NH_3)_z^+$) distributes the original signal intensity over the different reaction product ions, thus deteriorating the sensitivity, but improving the selectivity. In other words, higher sensitivity is to be expected when forming a single molecular ion after reaction in the cell, although the chance of still suffering from spectral interference also increases. By means of the formation of various molecular ions using highly reactive gases, the

signal intensity of each cluster ion is reduced, and thus also the sensitivity, but there is an increase of the probability of finding a reaction product ion free from spectral overlap. An example of such a situation is the interference-free determination of titanium (Ti) using O_2 or NH_3 in the CRC of an ICP-MS/MS instrument. The signal of the most abundant Ti isotope (48 amu, 73.8% abundance) overlaps with that of one of the Ca isotopes (48 amu, 0.187% abundance). Although. at first sight, the low abundance of ^{48}Ca may suggest that its contribution to the signal of $^{48}Ti^+$ could be considered negligible, it needs to be highlighted that Ca can be present at concentrations higher by several orders of magnitude compared to that of Ti, as is the case for biological samples. It can be noted that isobaric interferences like that of $^{48}Ti/^{48}Ca$ cannot be avoided using a non-reactive collision gas and kinetic energy discrimination, while the mass resolution required to separate the signal of both elements is much higher than that offered by present-day commercially available high-resolution sector field ICP-MS (HR-SF-ICP-MS) instrumentation. Thus, the formation of a Ti molecular ion upon selective ion-molecule chemistry in the CRC is an elegant way to avoid spectral overlap and to achieve interference-free conditions, but even this approach is not self-evident as a result of the analogous chemical behavior of both elements. The formation of TiO^+ and CaO^+ reaction products upon pressurizing the CRC with O_2 is an example of the difficulty of removing isobaric interferences, while it also shows the limited capabilities of gases predominantly forming diatomic reaction product ions for avoiding isobaric overlap. In contrast, the use of NH_3 leads to the formation of several cluster ions for both Ti ($Ti(NH_3)_x^+$; $x \leq 6$) and Ca ($Ca(NH_3)_x^+$; $x \leq 5$). Based on this slightly different reactivity, ^{48}Ti could be determined interference-free by monitoring the $^{48}Ti(NH_3)_6^+$ reaction product ion (m/z = 150) in the presence of very high Ca concentrations, as the number of NH_3

molecules coordinated around a Ca ion was found to be ≤5 (highest order reaction product ion for Ca is $Ca(NH_3)_5^+$, while for Ti, it is $^{48}Ti(NH_3)_6^+$) [132]. The development of this method further demonstrates the usefulness of PIS for determining the best suited reaction product ion when dealing with complex ion-molecule chemistry (see **Figure 6** for an example of PIS showing Ti-based and Ca-based reaction product ions with O_2 (a) and NH_3 (b)). Also, similarly to the determination of S, but even to a larger extent, the isotopic pattern of Ti has to be preserved to obtain accurate determinations. This can be achieved by using the first quadrupole as a 1-amu mass filter in MS/MS instrumentation, as otherwise, other Ti isotopes would not be filtered out and would overlap with the target isotope after reaction with NH_3 (*e.g.*, $^{49}Ti(NH_3)_5(NH_2)^+$ and $^{48}Ti(NH_3)_6^+$, both with m/z = 150 amu).

The ability to preserve the isotopic pattern is of the utmost importance in the context of isotopic analysis. As an example, interference-free Sr isotopic analysis with a sufficient isotope ratio precision for geo-applications such as Rb/Sr-dating without the need of Rb/Sr separation to avoid the spectral overlap of the isobars ^{87}Sr and ^{87}Rb was enabled by monitoring of the molecular reaction product ions of Sr instead of the corresponding atomic ions. While Hogmalm *et al.* compared the use of N_2O and SF_6 for this purpose [133], Bolea-Fernandez *et al*. suggested the use of CH_3F [134,135]. These approaches even enabled direct Sr isotopic analysis of solid samples by using laser ablation as a means of sample introduction (LA-ICP-MS/MS).

In addition to the use of a single reaction gas, the potential of chemical resolution to overcome spectral interferences can be extended by a combination of reaction gases, a situation that can be of interest for addressing isobaric ions showing a similar behavior towards a given reaction gas. An example of this situation is the

interference-free determination of vanadium (V). The most abundant V isotope (^{51}V, 99.75%) suffers from overlap with $^{35}Cl^{16}O^+$ ions and other polyatomic interferences, while the other V isotope (^{50}V, 0.25%) is affected by overlap with the signals of the isobars ^{50}Cr and ^{50}Ti, rendering a situation that, *e.g.*, prevented the use of isotope dilution (ID). Nonose *et al*. developed an ID-ICP-MS method for the selective determination of both V isotopes in the presence of Ti and Cr using a mixture of CH_3F and NH_3 in the CRC of an SQ-ICP-MS instrument [136]. This method was used for the analysis of fine ceramics containing high Cr and Ti contents and relied on the selective formation of $VF_2(NH_3)_4^+$ by controlling the gas flow rates of both reactive gases. More recently, the use of a combination of O_2 and H_2 in the CRC of an ICP-MS/MS instrument has been suggested for the determination of Ti as the reaction product ion TiO^+, while the CaO^+ polyatomic interference can be mass-shifted owing to the formation of $CaOH^+$ molecular ions [137].

From all of the above, it may seem that molecular ion monitoring is restricted to mono-element determinations, as a result of the specificity of some reaction gases towards a given target analyte. However, several works published to date have demonstrated the potential of chemical resolution and reaction product ion monitoring for multi-element determinations. For instance, Virgilio *et al*. studied the reactivity and analytical performance of O_2 as a cell gas in ICP-MS/MS and classified 18 elements according to their reactivities. While some target atomic ions were converted into molecular reaction product ions, for others it was the reaction of O_2 with the interfering species that provided interference-free conditions [138]. Bolea-Fernandez *et al*. evaluated the potential of the highly reactive CH_3F gas for the multi-element determination of medically relevant metals at ultra-trace concentrations in biofluids. The results demonstrated that a truly multi-element determination (using a single set

of conditions only) can be achieved by using a compromise gas flow rate without significantly affecting the figures-of-merit achieved for mono-element determinations [139,140].

Additionally to the use of molecular ion formation in the CRC to remove spectral overlap in mono- and multi-elemental analysis, an alternative idea that has been explored relatively recently deals with the formation of a molecular ion in the plasma, rather than in the CRC. This approach has been used for the ICP-MS determination of fluorine (F), an element that can theoretically not even be determined using ICP-MS as its ionization energy is higher than that of the plasma gas Ar (17.42 vs. 15.76 eV), but that is of the utmost interest due to the presence of F in approximately 20% of today's pharmaceutical drugs. The method consists of bypassing the issue of low ionization yields for F by using a molecule-forming agent, an approach that resembles that described in the previous sections for molecular absorption or emission spectroscopies. Different elements were studied for their utility as molecule-forming agent in this work, but the introduction of a barium (Ba) solution and the monitoring of the molecular ion $^{138}Ba^{19}F^{+}$ formed in the ICP provided the best results [141]. The method developed enabled total F determination with acceptable LODs and reproducibility, although a second work from the same authors argued that the robustness of the method can be affected by matrix effects, thus giving an argument for the development of negative mode ICP-MS [75].

Another example of molecular ion monitoring for purposes different than removing spectral overlap in ICP-MS was reported by Williams *et al.* [142]. In this work, the authors take advantage of the ion-molecule chemistry occurring within the CRC of an ICP-MS/MS instrument to suggest a novel calibration approach. The method, called

multi-species calibration (MSC), relies on the use of various molecular ion species (different m/z ratios) from the same target analyte instead of several standard solutions and a single m/z ratio [143]. For this purpose, two calibration solutions containing (*i*) a 1:1 mixture of sample and a standard solution (S1) and (*ii*) a 1:1 mixture of the sample and a blank solution (S2) were measured for multiple oxide and ammonia cluster species of the target analyte. This approach resembles the multi-isotope calibration (MICal) approach, although in the latter, different isotopes from the same element, instead of various reaction product ions, are measured [144]. The calibration curve was built by plotting the signals of S1 *versus* those of S2. Thus, the analyte concentration in the sample can be determined based on the relationship between instrument responses from multiple "channels" recorded for solutions containing the same matrix, thus making this approach virtually free from matrix effects. Also, this novel calibration method overcomes one of the major limitations of MICal approach, as it can be applied to mono-isotopic elements as well. The MSC calibration method proved to be accurate and precise for the determination of As, Co and Mn in CRMs of environmental and biological origin. An additional advantage of the MSC is the easy identification of spectral overlap for the molecular ions monitored, as the linearity of the calibration curve would be affected in the presence of interferences.

Moreover, the ability to monitor the reactivity of different atomic ions towards a selected gas has also been exploited for the purpose of studying the catalytic properties of different elements [145]. In this work, the possibility of using the CRC of an ICP-MS/MS instrument as a catalytic reactor for methane activation was investigated. 37 elements commonly used as gaseous catalysts were screened by fixing the m/z ratio of Q1 (the one of the target element of interest) and identifying the

different reaction product ions formed upon reaction with CH_4 in the cell by scanning Q2. The results demonstrated that this approach can be effectively used for a high-throughput screening of the catalytic properties of various elements.

4.4. Drawbacks and remaining challenges

Undoubtedly, the use of chemical resolution and molecular ion monitoring is an approach of growing interest in the field of ICP-MS, especially since the introduction of mass spectrometers with tandem (MS/MS) configuration, offering better control over the ion-molecule processes occurring within the CRC. However, some challenges still remain when using this approach to overcome spectral overlap.

Despite recent developments in this field, the use of a higher mass resolution offered by SF-ICP-MS instrumentation is still a more straightforward and universal approach to overcome spectral overlap in ICP-MS, especially when aiming at multi-elemental analysis with a single set of analysis parameters, independent of the sample matrix and with limited method development only [146]. Self-evidently, insufficient mass resolving power to avoid certain types of spectral overlap and a reduction in ion transmission efficiency, and thus sensitivity, when operating at higher mass resolution, have to be pointed out as major limitations of SF-ICP-MS instrumentation. Despite high mass resolution still providing an easier approach for overcoming spectral overlap, ICP-MS/MS technology has largely bridged the gap between sector field and quadrupole-based ICP-MS instrumentation, but it should not get unnoticed that method development based on the use of chemical resolution and molecular ion monitoring is quite demanding compared to switching from low to higher mass resolution in SF-ICP-MS. As indicated above, a proper gas needs to be selected, the ion-molecule reactions occurring in the cell need to be identified and

several settings, like gas flow rate and mass window (quadrupole-based CRC only) and/or retardation potential, need to be carefully optimized. Also, the use of chemical resolution generally involves a subtle balance between sensitivity and selectivity, so that interference-free conditions can still be achieved without sacrificing detection capabilities. Attention must also be paid to potential undesired side reactions giving rise to unwanted molecular ions overlapping with the target reaction product ion, thus preventing interference-free determination.

For multi-element ("panoramic") trace analysis, different modes of operation, involving not only much more method development, but also various gas mixtures, are typically needed. As a result, the time required to change from one set of conditions to the next, including the stabilization of the CRC conditions after introduction of another gas, must be considered. Thus, applications requiring multi-element monitoring at high speed, such as low sample volume analysis or laser ablation ICP-MS imaging, can be compromised to a larger extent than with traditional scanning-type quadrupole based ICP-MS instrumentation operated in "no gas" or cell-vented mode.

Moreover, the use of some reaction gases affects the capability to obtain fast temporally resolved information, as encountered during single-event analysis (*i.e.* single-particle and single-cell ICP-MS). This approach aims at detecting and quantifying the analyte content of small entities, such as nanoparticles and individual cells and is nowadays one of the emerging topics in the field of ICP-MS. It has been demonstrated that the use of ICP-QMS combined with CRC technology compromises this approach, as the short transient signals generated by the burst of ions produced whenever a single nanoparticle reaches the ICP (and with an average signal duration of approximately 0.5 ms under normal conditions) are affected by interactions of the

ion cloud with the cell gas(es) [147]. This results in a longer signal duration for each individual event and thus, in poorer detection capabilities.

Last but not least, chemical resolution often requires the use of hazardous gases, thus requiring a more complicated instrument setup and the necessary safety measures (*e.g.*, gas detectors) in order to reduce the risks associated with some corrosive, flammable and/or explosive gases or gas mixtures.

5. Perspectives and future directions

Overall, the approach described in this review, which could be described as a type of on-measurement derivatization, since it typically does not require any extra sample pretreatment, offers intriguing new options (such as isotopic analysis using optical techniques) and new ways to determine challenging analytes and, in particular, non-metals.

In the case of the optical techniques, what can be expected in the future is to make more use of the potential to combine molecular and atomic spectra. In the case of MAS, this requires the use of instrumentation with much wider spectral windows, which is already technically possible, as clearly demonstrated by Geisler *et al*. [73] and Labusov *et al*. [74]. In the case of LIBS, this is also possible, but there is another interesting trend to consider: combining both LIBS/LAMIS and LA-ICP-MS(/MS) information from the same ablation process [148]. Experimenting with data fusion appears as a logical step in this research area.

What seems clear is that molecules should not be neglected as target species when aiming at obtaining trace elemental and isotopic information.

Acknowledgements

The authors acknowledge the following projects: PGC2018-093753-B-I00 (MCIU/AEI//FEDER, UE); CTQ2015-64684P (MINECO/FEDER); the European Regional Development Fund for financial support through Interreg POCTEFA 176/16/ DBS; the Aragon Government (Construyendo Europa desde Aragón); CTQ2016-77887-C2-1-R; GRUPIN-IDI/2018/000186. E. Bolea-Fernandez thanks FWO-Vlaanderen for his postdoctoral grant.

Conflicts of interest: none

Table 1. Most representative emission system for the CaF and CaCl molecular emission in the UV-VIS spectral region.

Molecule	System	Wavelength range
CaF	$A^2\Pi - X^2\Sigma$	583.0 – 630.0 nm (Orange System)
	$B^2\Sigma - X^2\Sigma$	514.0 – 543.0 nm (Green System)
CaCl	$A^2\Pi - X^2\Sigma$	604.7 – 636.1 nm (Red System)
	$B^2\Sigma - X^2\Sigma$	581.0 – 606.7 nm (Orange System)

Table 2. Examples of isotopic analysis using LAMIS, including information about the employed isotopes, molecules, electronic system and molecular bands and, and observed isotopic shift (e.g. the sign in the isotopic shift corresponds to the subtraction of the bandhead wavelengths of heavier isotope minus lighter isotope).

Element	**Molecule**	**Electronic System and Vibrational Band**	**Shift (nm)**	**Ref**
^{10}B-^{11}B	BO	$X^2\Sigma^+ - B^2\Sigma^+$ (0,2)	-0.73	[6]
H-D	OH	$A^2\Sigma^+ - X^2\Pi_i$ (0,0)	-0.68	[6]
^{12}C-^{13}C	C_2	$d^3\Pi_g - a^3\Pi_u$ (0,0)	-0.03	[6]
^{12}C-^{13}C	CN	$B^2\Sigma^+ - X^2\Sigma^+$ (0,0)	0.03	[6]
^{86}Sr-^{88}Sr	SrO	$A^1\Sigma^+ - X^1\Sigma^+$ (2,0)	0.15	[47]
^{235}U-^{238}U	UO	(593.55 nm band)	0.04	[48]
^{14}N-^{15}N	CN	$B^2\Sigma^+ - X^2\Sigma^+$ (0,1)	-0.7	[53]
^{16}O-^{18}O	AlO	$B^2\Sigma^+ - X^2\Sigma^+$ $(\Delta v = +1)$		[49]
^{90}Zr-^{94}Zr	ZrO	$d^3\Delta_3 - a^3\Delta_3$ (0,1)	-0.08	[50]
^{35}Cl-^{36}Cl	CaCl	$B^2\Sigma^+ - X^2\Sigma^+$ $(\Delta v = -1)$		[49]

Table 3. Selected applications reporting on the use of HR CS MAS.

Vaporizer	Analyte	Species monitored	λ (nm)	LOD / m_0	Sample	Ref.
Graphite furnace	Br	BaBr	520.819	1.7 ng / 4.0 ng	Pharmaceuticals	[149]
Graphite furnace	Br	AlBr CaBr	278.914 625.315	2 ng / N.A. 2 ng / N.A.	Salt and pharmaceutical product	[150]
Graphite furnace	Br	CaBr	625.315 625.223 625.135 625.058	5.4 ng / 1.32 ng 7.3 ng / 1.77 ng 12.7 ng / 2.42 ng 18.2 ng / 3.00 ng	6 polymeric CRMs	[77]
Graphite furnace	Br	TlBr	342.982	0.3 ng / 4.4 ng	Water	[151]
Flame	Cl	InCl	267.24	3 mg L^{-1} / N.A.	BCR151 (Milk powder), HISS-1 and PACS-2 (Marine sediments)	[152]
Graphite furnace	Cl	AlCl	261.42	70 pg/ 300 pg	Rye flour CRM	[68]
Graphite furnace	Cl	AlCl InCl SrCl	261.418 267.281 635.862	2.1 ng / 0.28 ng 3.5 ng / 1.7 ng 0.7 ng / 1.0 ng	NIST 1634c fuel oil, Crude oil	[153]
Graphite furnace	Cl	CaCl	620.862 377.501	0.75 ng / 0.072 ng 14.2 ng / 25.9 ng	CRMs of different nature	[154]
Graphite	Cl	GaCl	249.060	2.3 ng / 6.5 ng	Milk and mineral water and	[155]

furnace					a certified wastewater sample	
Graphite furnace	Cl	MgCl	377.010	1.7 ng / 7.1 ng	Water samples from offshore oil wellbore and several CRMs (steam coal and bovine muscle powder)	[156]
Graphite furnace	Cl	SrCl	635.862	0.85 ng / 0.24 ng	Coal (5 CRMs)	[157]
Flame	F	GaF	211.248	1 mg L^{-1} / N.A.	BCR33 (Super-phosphate)	[158]
Flame	F	AlF	227.461	5.5 mg L^{-1} / 72.8 mg L^{-1}	Toothpaste and wastewater	[159]
Graphite furnace	F	CaF	606.440	1.6 ng / 2.5 ng	Tea	[160]
Graphite furnace	F	GaF	211.248	9 pg / 13 pg	CRMs BCR 109 (Zinc ore) and BCR 274 (single cell protein)	[68]
Graphite furnace	F	SrF	651.187	0.36 ng / 0.55 ng	Water	[161]
Graphite furnace	I	BaI CaI InI SrI	538.304 638.892 400.472 677.696	60 ng / 17 ng 180 ng / 22 ng 120 ng / 14 ng 66 ng / 2 ng	Iodine and levothyroxine supplement samples	[89]
Graphite furnace	I	CaI SrI	638.904 677.692	0.041 mg g^{-1} / 23 ng 0.021 mg g^{-1} / 18 ng	Medicines	[88]
Graphite furnace	Nitric acid	NO	214.526 214.587	N.A. / 10 pg N.A. / 10 pg	Water CRMs and a nitrate fertilizer CRM	[92]

			214.744 214.904 215.195 215.360	N.A. / 8 pg N.A. / 7 pg N.A. / 11 pg 5 ng N / 7 pg		
Graphite furnace	Nitric acid	NO	215.360	96 ng / 20 ng	Etching solutions of silicon wafers	[162]
Flame	P	P PO PO PO PO PO	213.618 246.400 247.620 247.780 324.616 327.040	55 mg L^{-1} / 140 mg L^{-1} 20 mg L^{-1} / 128 mg L^{-1} 17 mg L^{-1} / 192 mg L^{-1} 12 mg L^{-1} / 173 mg L^{-1} 18 mg L^{-1} / 217 mg L^{-1} 20 mg L^{-1} / 233 mg L^{-1}	Liquid fertilizer and NIST 120c phosphate rock	[163]
Flame	P	PO	246.400 247.620 247.780	27.2 mg L^{-1} / 211.3 mg L^{-1} 16.4 mg L^{-1} / 251.1 mg L^{-1} 39.3 mg L^{-1} / 358.0 mg L^{-1} Σ=15.6 mg L^{-1} /135 mg L^{-1}	Plants	[164]
Graphite furnace	P	PO	246.40	0.9 ng / 4.4 ng	Rye flour CRM	[68]
Graphite furnace	P	P PO	213.618 213.508 213.561 213.580 213.587 213.616 213.635 213.646 213.674	4.9 µg g^{-1} / 4.6 ng Σ=20.8 µg g^{-1} / 4.7 ng	Biological CRMs	[165]

			213.694			
Graphite furnace	P	P_2	204.205	7 ng / 10 ng	Biological and clinical reference materials	[166]
Flame	S	CS	257.593 257.959 258.056	4.4 mg L^{-1} / 90 µg g^{-1} N.A. / 120 µg g^{-1} 2.4 mg L^{-1} / 125 µg g^{-1}	Cast iron CRMs	[167]
Flame	S	CS SH	257.595 257.958 258.056 323.658 324.064 327.990	13.4 mg L^{-1} / 393.9 mg L^{-1} 22.5 mg L^{-1} / 412.5 mg L^{-1} 30.0 mg L^{-1} / 400.3 mg L^{-1} 2.80 g L^{-1} / 10.8 g L^{-1} 1.70 g L^{-1} / 13.1 g L^{-1} 0.78 g L^{-1} / 5.17 g L^{-1}	Fungicides and fertilizers	[168]
Graphite furnace	S	CS	258.056	2.3 ng / 12 ng	Biological CRMs	[68]
Graphite furnace	S	CS	257.958 257.850 257.864 257.908 258.033 258.056	9 ng / 14 ng	Polymer, steel, petroleum, coke and biological CRMs	[69]
Graphite furnace	S	SnS	271.624	5.8 ng / 13.3 ng	Crude oil (CRMs)	[169]
Graphite furnace	S	GeS PbS SiS	295.209 335.085 282.910	-- / 9.4 ng -- / 220 ng -- / 15.7 ng		[170]

		SnS	271.578	-- / 20 ng		

Table 4. Applications reporting on the use of HR CS MAS for isotopic analysis in order of publication. In all cases, a graphite furnace was used as vaporizer.

Analyte	**Species monitored**	**λ (nm)**	**Sample**	**Reference**
Cl	$Al^{35}Cl$ $Al^{37}Cl$	262.238 262.222	CRMs with certified Cl isotopic composition CRMs of water and commercial mineral waters	[83]
Br	$Ca^{79}Br$ $Ca^{81}Br$	600.492 600.467	Reference materials: PVC and tomato leaves	[85]
B	^{10}BH ^{11}BH	Different lines around 433.1 and 437.1 nm	Certified isotope reference materials and boron solutions	[86]
Ca	^{40}CaF ^{44}CaF	628.534 628.191	Urine samples spiked with ^{40}Ca and ^{44}Ca	[87]

Table 5. Selected applications relying on the use of chemical resolution and molecular ion monitoring using ICP-MS/MS.

CRC gas	Reactions	Analyte	Molecular ion(s) monitored	Sample	Ref.
H_2	$M^+ + H_2 \rightarrow MH_2^+$	Cl	ClH_2^+	Foods, sediments, biofluids, pharmaceuticals, crude oils	[125], [130], [131], [171,172], [173]
O_2	$M^+ + O_2 \rightarrow MO^+ + O^+$	Si	SiO^+	Biodiesel	[124]
		P	PO^+	Peptides, biodiesel, foods, tissues, cells, pharmaceuticals, proteins	[122], [124], [125], [127], [128], [171], [174]
		S	SO^+	Peptides, biodiesel, foods, organic matrices, cells, pharmaceuticals, proteins, beverages, quantum dots	[122], [124], [125], [126], [128], [171], [174-176], [177,178], [179]
		As	AsO^+	Foods, cells	[180-185], [128]
	$M^+ + O_2 \rightarrow MO_2^+$	Si	SiO_2^+	Nuclear waste glasses	[186]
		Mo	MoO_2^+	Standard solutions, Milk	[138], [187]
N_2O	$M^+ + N_2O \rightarrow MO^+ + N_2$	Sr	SrO^+	Minerals	[133]
		Ra	RaO^+	Water and geological samples	[188]

NH_3	$M^+ + NH_3 \rightarrow MNH_x(NH_3)_y^+$	Ti	$TiNH(NH_3)_4^+$	Quartz	[189]
		Ir	$IrNH^+$	Standard solutions	[190]
		Os	$OsNH^+$	Standard solutions	[190]
	$M^+ + NH_3 \rightarrow M(NH_3)_x^+$	Ti	$Ti(NH_3)_6^+$	Biofluids, nanoparticles	[132], [191]
		Fe	$Fe(NH_3)_2^+$	Crude oils	[192]
		Pd	$Pd(NH_3)_3^+$	Moss samples	[193]
		Pt	$Pt(NH_3)_2^+$	Standard solutions, moss samples	[190], [193]
CH_3F	$M^+ + CH_3F \rightarrow M(CH_3F)_x^+$	Co, Cr, Ni	$Co(CH_3F)_2^+$, $Cr(CH_3F)_2^+$, $Ni(CH_3F)_2^+$	Biofluids	[139,140]
		Mn	$Mn(CH_3F)^+$	Biofluids	[139]
	$M^+ + CH_3F \rightarrow MF_x(CH_3F)_y^+$	Sr	SrF^+	Biofluids, geological samples	[140], [134,135]
		Zr	ZrF^+	Biofluids	[140]
		Ti, V	$TiF_2(CH_3F)_3^+$, $VF_2(CH_3F)_3^+$	Biofluids	[139,140]
	$M^+ + CH_3F \rightarrow MCH_2(CH_3F)_y^+ + HF$	As, Se	$AsCH_2^+$, $SeCH_2^+$	Environmental samples	[194]
	$M^+ + CH_3F \rightarrow MCHF(CH_3F)_y^+ + H_2$	Pt	$PtCHF^+$	Road dust	[195]
SF_6	$M^+ + SF_6 \rightarrow MF_x^+ + SF_{6-x}$	Ca, Sr	CaF^+, SrF^+	Minerals	[133]

Figure captions

Figure 1: **A)** Spectra showing the CaCl molecular emission for different amounts of $CaCl_2$ in the sample. Reproduced with permission of Elsevier (https://doi.org/10.1016/j.icarus.2017.12.006) [37]; **B)** CaF molecular emission from samples without F and Ca (Sample A), only with Ca (Sample B) and containing both elements (Sample C). Reproduced with permission of Elsevier https://doi.org/10.1016/j.sab.2016.08.006 [34]; **C)** Scheme of the experimental set-up used for the analysis of Ca-free samples in order to obtain the CaF molecule. Reproduced with permission of the RSC (https://doi.org/10.1039/C6JA00386A) [35].

Figure 2: **A)** Comparison between the molecular and the atomic isotopic shift. Reproduced with permission of Elsevier (https://doi.org/10.1016/j.sab.2011.01.007) [6]. **B)** Emission of the $A^1\Sigma^+ - X^1\Sigma^+$ SrO system showing the isotopic shift in the head bands. Reproduced with permission of Elsevier https://doi.org/10.1016/j.sab.2011.12.002) [47].

Figure 3. A) Time and wavelength resolved CS absorbance spectrum obtained in the vicinity of 258 nm upon vaporization of 500 ng of sulfur by means of HR CS GF MAS. Reproduced with permission of the RSC (https://doi.org/10.1039/C2JA10322B) [69]. **B)** Time and wavelength resolved CaBr absorbance spectrum obtained in the vicinity of 625 nm upon vaporization of 100 pg of Br in the presence of excess of Ca. Reproduced with permission of Elsevier (https://doi.org/10.1016/j.sab.2013.07.013) [77].

Figure 4. Spectra of AlCl upon vaporization of 400 ng of Cl from an aqueous solution with a $^{35}Cl/^{37}Cl$ molar ratio of approximately 1:1, in the presence of excess of Al and Pd, as measured *via* HR CS GF MAS [83].

Figure 5. Schematic overview of a tandem ICP-mass spectrometer operated in MS/MS mode. The design shows two quadrupole mass filters with a CRC located in-between. The example selected illustrates the interference-free determination of $^{35}Cl^+$ (m/z Q1 = 35 amu) by monitoring the reaction product ion $^{35}ClH_2^+$ (m/z Q2 = 37 amu), whereby all concomitant matrix ions (including $^{37}Cl^+$) are efficiently removed by means of Q1.

Figure 6: Example of product ion scanning for the selection of the best suited Ti-based reaction product ions with O_2 (**A)** and NH_3 (**B)**. PIS is a powerful tool for the identification of the molecular ions formed upon reaction in the cell; the different products are shown as a function of their m/z ratio in the Q2 full mass spectrum (2 – 260 amu, x-axis) when monitoring either a 1 µg L^{-1} Ti solution (blue bars) or a solution containing 1 µg L^{-1} Ti plus 10 mg L^{-1} Ca (red bars). Adapted from [132] (https://doi.org/10.1016/j.aca.2013.10.017) with permission of Elsevier.

Figure 1

A

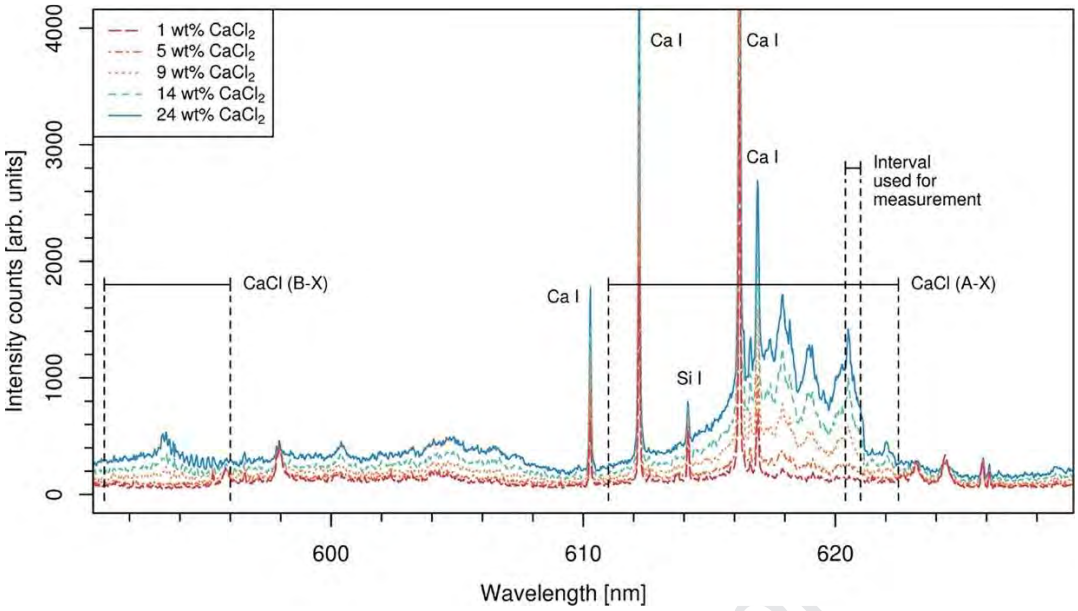
1 wt% CaCl2
5 wt% CaCl2
9 wt% CaCl2
14 wt% CaCl2
24 wt% CaCl2
Ca I
Ca I
Ca I
Interval used for measurement
CaCl (B-X)
Ca I
CaCl (A-X)
Si I
Intensity counts [arb. units]
Wavelength [nm]

B

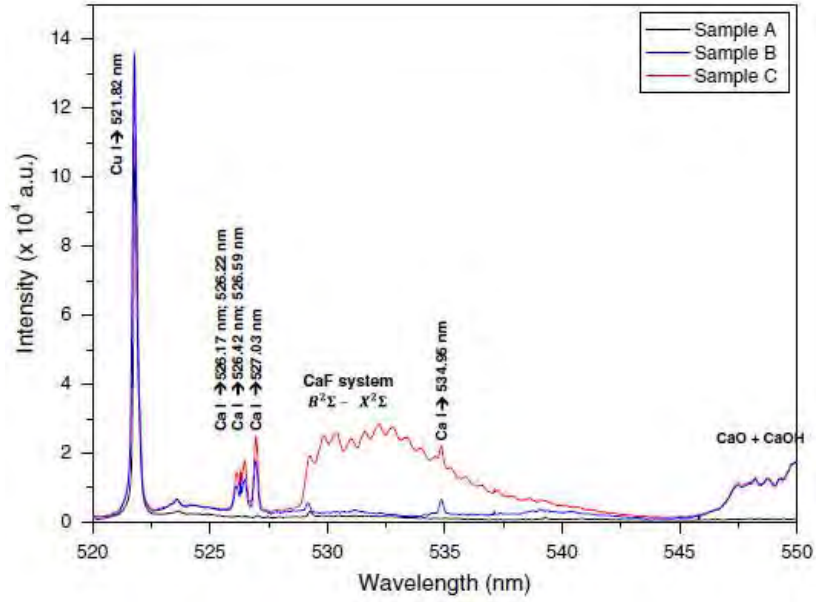
Sample A
Sample B
Sample C
Cu I → 521.82 nm
Ca I → 526.17 nm; 526.22 nm
Ca I → 526.42 nm; 526.59 nm
Ca I → 527.03 nm
CaF system
B²Σ - X²Σ
Ca I → 534.96 nm
CaO + CaOH
Intensity (x 10⁴ a.u.)
Wavelength (nm)

C

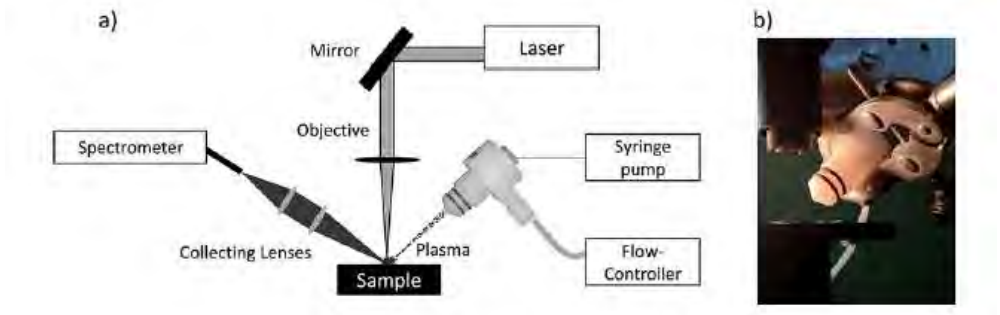
a)
Mirror
Laser
Objective
Spectrometer
Syringe pump
Collecting Lenses
Plasma
Sample
Flow-Controller
b)

Figure 2

A

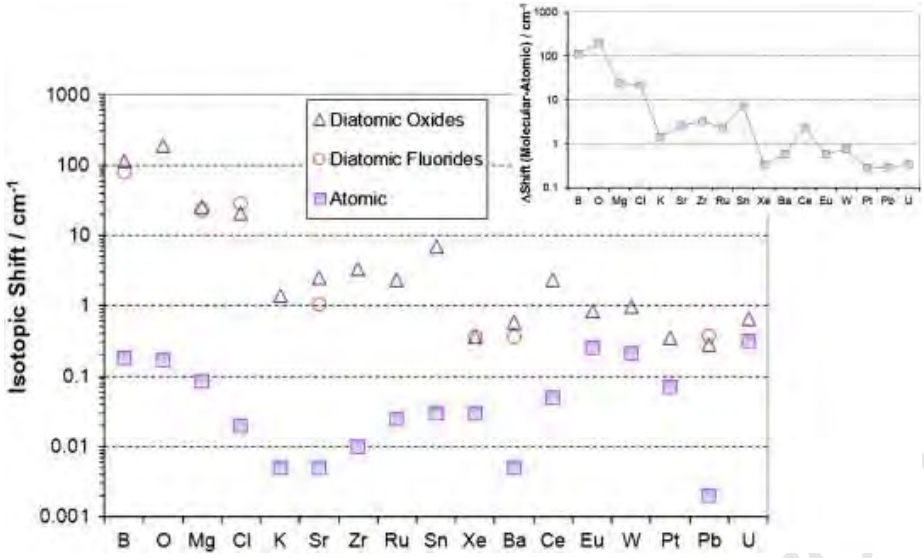
Isotopic Shift / cm-1
1000
100
10
1
0.1
0.01
0.001
B O Mg Cl K Sr Zr Ru Sn Xe Ba Ce Eu W Pt Pb U
Diatomic Oxides
Diatomic Fluorides
Atomic
ΔShift (Molecular-Atomic) / cm-1

B

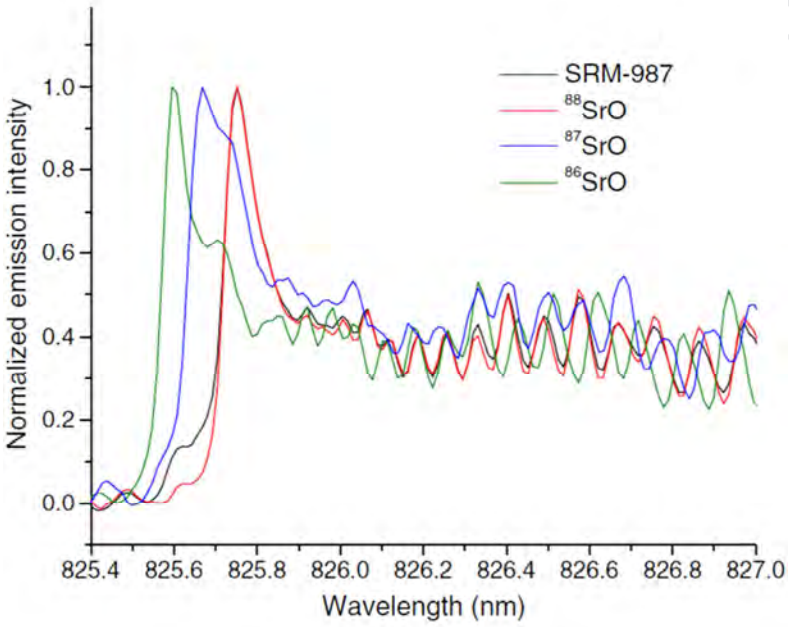
Normalized emission intensity
1.0
0.8
0.6
0.4
0.2
0.0
825.4 825.6 825.8 826.0 826.2 826.4 826.6 826.8 827.0
Wavelength (nm)
SRM-987
88SrO
87SrO
86SrO

Figure 3

a)

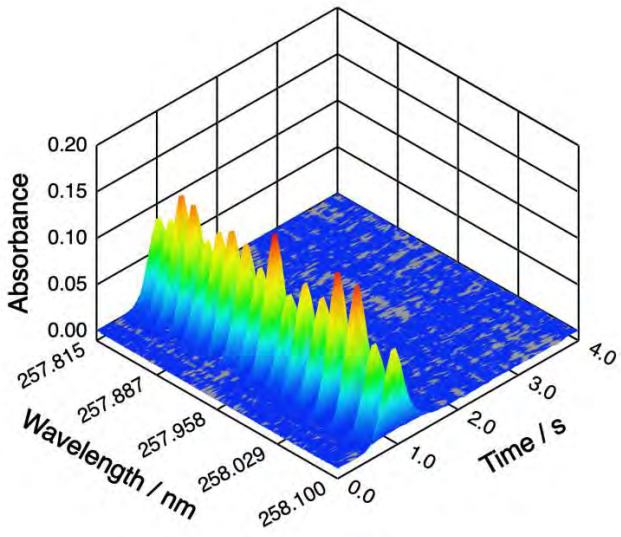
Absorbance
0.20
0.15
0.10
0.05
0.00
257.815
257.887
257.958
258.029
258.100
Wavelength / nm
0.0
1.0
2.0
3.0
4.0
Time / s

b)

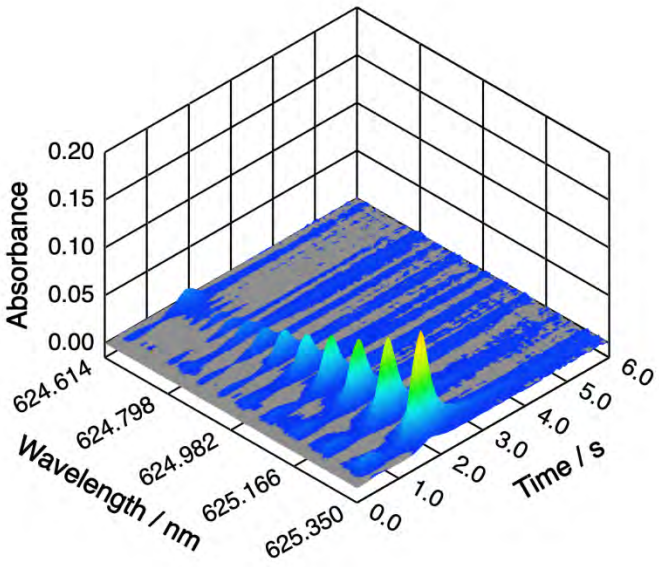
Absorbance
0.20
0.15
0.10
0.05
0.00
624.614
624.798
624.982
625.166
625.350
Wavelength / nm
0.0
1.0
2.0
3.0
4.0
5.0
6.0
Time / s

Figure 4

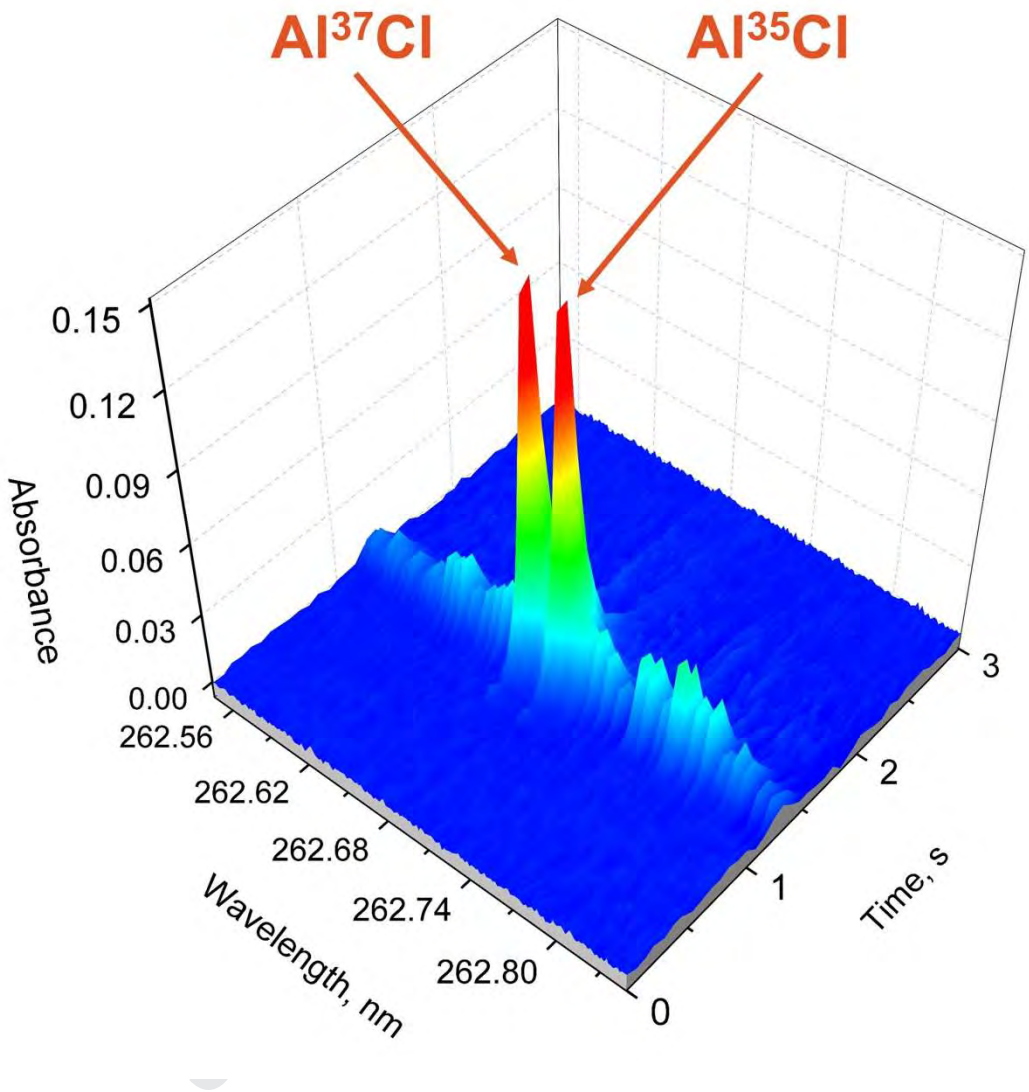
Al37Cl
Al35Cl
Absorbance
0.15
0.12
0.09
0.06
0.03
0.00
262.56
262.62
262.68
262.74
262.80
Wavelength, nm
0
1
2
3
Time, s

Figure 5

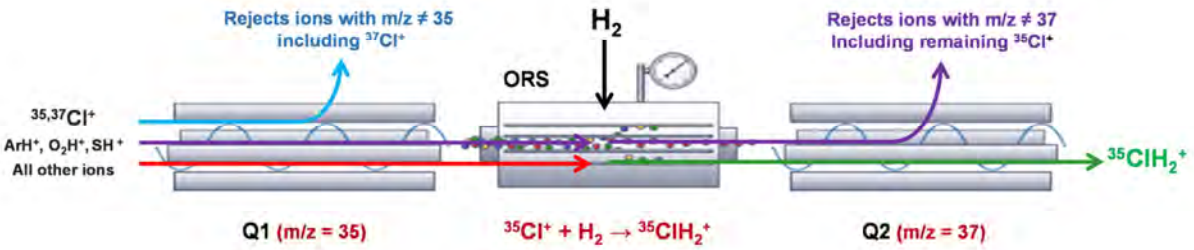

Figure 6

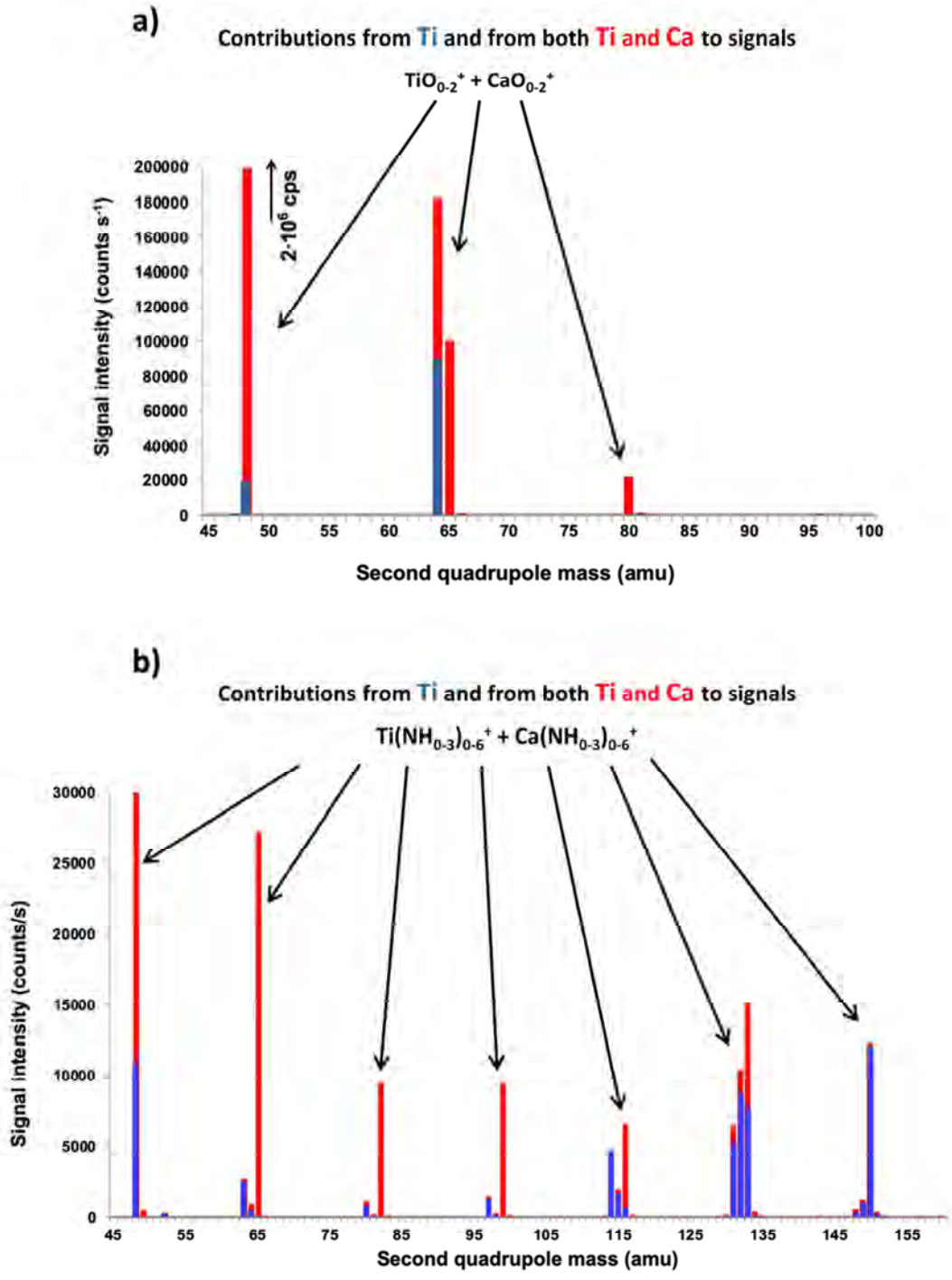
a)
Contributions from Ti and from both Ti and Ca to signals
$TiO_{0-2}^+ + CaO_{0-2}^+$
$2 \cdot 10^6$ cps
Signal intensity (counts s^{-1})
Second quadrupole mass (amu)
b)
Contributions from Ti and from both Ti and Ca to signals
$Ti(NH_{0-3})_{0-6}^+ + Ca(NH_{0-3})_{0-6}^+$
Signal intensity (counts/s)
Second quadrupole mass (amu)

References

[1] F. Vanhaecke, A new scope for JAAS!, J. Anal. At. Spectrom. 30 (2015) 1015–1016. https://doi.org/10.1039/C5JA90018B.
[2] A. Walsh, The development of atomic absorption methods of elemental analysis 1952-1962, Anal. Chem. 63 (1991) 933A-941A. https://doi.org/10.1021/ac00019a723.
[3] B. Welz, Atomic absorption spectrometry — pregnant again after 45 years, Spectrochim. Acta, Part B 54 (1999) 2081–2094. https://doi.org/10.1016/S0584-8547(99)00154-8.
[4] B. Welz, F.G. Lepri, R.G.O. Araujo, S.L.C. Ferreira, M.D. Huang, M. Okruss, H. Becker-Ross, Determination of phosphorus, sulfur and the halogens using high-temperature molecular absorption spectrometry in flames and furnaces–A review., Anal. Chim. Acta 647 (2009) 137–148. https://doi.org/10.1016/j.aca.2009.06.029.
[5] M. Resano, E. García-Ruiz, M. Aramendía, M.A. Belarra, *Quo vadis* high-resolution continuum source atomic/molecular absorption spectrometry?, J. Anal. At. Spectrom. 34 (2019) 59–80. https://doi.org/10.1039/C8JA00256H.
[6] R.E. Russo, A.A. Bol'shakov, X. Mao, C.P. McKay, D.L. Perry, O. Sorkhabi, Laser Ablation Molecular Isotopic Spectrometry, Spectrochim. Acta, Part B 66 (2011) 99–104. https://doi.org/10.1016/j.sab.2011.01.007.
[7] D.W. Hahn, N. Omenetto, Laser-Induced Breakdown Spectroscopy (LIBS), Part I: Review of Basic Diagnostics and Plasma-Particle Interactions: Still-Challenging Issues Within the Analytical Plasma Community, Appl. Spectrosc. 64 (2010) 335A-366A. https://doi.org/10.1366/000370210793561691.
[8] D.W. Hahn, N. Omenetto, Laser-Induced Breakdown Spectroscopy (LIBS), Part II: Review of Instrumental and Methodological Approaches to Material Analysis and Applications to Different Fields, Appl. Spectrosc. 66 (2012) 347–419. https://doi.org/10.1366/11-06574.
[9] J. Debras-Guédon, N. Liodec, De l'utilisation du faisceau issu d'un amplificateur à ondes lumineuses par émission induite de rayonnement (laser à rubis), comme source énérgetique pour l'excitation des spectres d'émission des éléments, C. R. Hebd. Seances Acad. Sci. 257 (1963) 3336–3339.
[10] J. Serrano, J. Moros, J.J. Laserna, Molecular signatures in femtosecond laser-induced organic plasmas: comparison with nanosecond laser ablation, Phys. Chem. Chem. Phys. 18 (2016) 2398–2408. https://doi.org/10.1039/C5CP06456B.
[11] V.S. Burakov, N.V. Tarasenko, N.A. Savastenko, Plasma chemistry in laser ablation processes, Spectrochim. Acta, Part B 56 (2001) 961–971. https://doi.org/10.1016/S0584-8547(01)00192-6.
[12] A. De Giacomo, J. Hermann, Laser-induced plasma emission: from atomic to molecular spectra, J. Phys. D: Appl. Phys. 50 (2017) 183002. https://doi.org/10.1088/1361-6463/aa6585.
[13] S. Grégoire, V. Motto-Ros, Q.L. Ma, W.Q. Lei, X.C. Wang, F. Pelascini, F. Surma, V. Detalle, J. Yu, Correlation between native bonds in a polymeric material and molecular emissions from the laser-induced plasma observed with space and time resolved imaging, Spectrochim. Acta, Part B 74–75 (2012) 31–37. https://doi.org/10.1016/j.sab.2012.07.020.
[14] X.K. Shen, H. Wang, Z.Q. Xie, Y. Gao, H. Ling, Y.F. Lu, Detection of trace phosphorus in steel using laser-induced breakdown spectroscopy combined with laser-induced fluorescence, Appl. Opt. 48 (2009) 2551–2558. https://doi.org/10.1364/AO.48.002551.
[15] C. González de Vega, C. Álvarez Llamas, N. Bordel, R. Pereiro, A. Sanz-

Medel, Analytical potential of a laser ablation-glow discharge-optical emission spectrometry system for the analysis of conducting and insulating materials, Anal. Chim. Acta 877 (2015) 33–40. https://doi.org/10.1016/j.aca.2015.04.034.
[16] M. Gaft, L. Nagli, I. Fasaki, M. Kompitsas, G. Wilsch, Laser-induced breakdown spectroscopy for on-line sulfur analyses of minerals in ambient conditions, Spectrochim. Acta, Part B 64 (2009) 1098–1104. https://doi.org/10.1016/j.sab.2009.07.010.
[17] M. Tran, Q. Sun, B.W. Smith, J.D. Winefordner, Determination of F, Cl, and Br in Solid Organic Compounds by Laser-Induced Plasma Spectroscopy, Appl. Spectrosc. 55 (2001) 739–744. https://doi.org/10.1366/0003702011952433.
[18] M. Tran, B.W. Smith, D.W. Hahn, J.D. Winefordner, Detection of Gaseous and Particulate Fluorides by Laser-Induced Breakdown Spectroscopy, Appl. Spectrosc. 55 (2001) 1455–1461. https://doi.org/10.1366/0003702011953865.
[19] S. Eto, T. Matsuo, T. Matsumura, T. Fujii, M.Y. Tanaka, Quantitative estimation of carbonation and chloride penetration in reinforced concrete by laser-induced breakdown spectroscopy, Spectrochim. Acta, Part B 101 (2014) 245–253. https://doi.org/10.1016/j.sab.2014.09.004.
[20] S. Millar, C. Gottlieb, T. Günther, N. Sankat, G. Wilsch, S. Kruschwitz, Chlorine determination in cement-bound materials with Laser-induced Breakdown Spectroscopy (LIBS) – A review and validation, Spectrochim. Acta, Part B 147 (2018) 1–8. https://doi.org/10.1016/j.sab.2018.05.015.
[21] C. Gottlieb, S. Millar, T. Günther, G. Wilsch, Revealing hidden spectral information of chlorine and sulfur in data of a mobile Laser-induced Breakdown Spectroscopy system using chemometrics, Spectrochim. Acta, Part B 132 (2017) 43–49. https://doi.org/10.1016/j.sab.2017.04.001.
[22] J. Bengoechea, E.T. Kennedy, Time-integrated, spatially resolved plasma characterization of steel samples in the VUV, J. Anal. At. Spectrom. 19 (2004) 468–473. https://doi.org/10.1039/B315653B.
[23] G. Asimellis, A. Giannoudakos, M. Kompitsas, New near-infrared LIBS detection technique for sulfur, Anal. Bioanal. Chem. 385 (2006) 333–337. https://doi.org/10.1007/s00216-006-0345-1.
[24] A. Hrdlička, J. Hegrová, K. Novotný, V. Kanický, D. Prochazka, J. Novotný, P. Modlitbová, L. Sládková, P. Pořízka, J. Kaiser, Sulfur determination in concrete samples using laser-induced breakdown spectroscopy and limestone standards, Spectrochim. Acta, Part B 142 (2018) 8–13. https://doi.org/10.1016/j.sab.2018.01.015.
[25] X. Zhang, Y. Deguchi, Z. Wang, J. Yan, J. Liu, Sensitive detection of iodine by low pressure and short pulse laser-induced breakdown spectroscopy (LIBS), J. Anal. At. Spectrom. 29 (2014) 1082–1089. https://doi.org/10.1039/C4JA00044G.
[26] D.A. Cremers, L.J. Radziemski, Detection of chlorine and fluorine in air by laser-induced breakdown spectrometry, Anal. Chem. 55 (1983) 1252–1256. https://doi.org/10.1021/ac00259a017.
[27] S. Datta, A. Fowler, On the spectra of the alkaline earth fluorides and their relation to each other, Proc. R. Soc. A. 99 (1921) 436–455. https://doi.org/10.1098/rspa.1921.0057.
[28] J. Papish, L.E. Hoag, W.E. Snee, Spectroscopic Detection of Fluorine, Ind. Eng. Chem. Anal. Ed. 2 (1930) 263–264. https://doi.org/10.1021/ac50071a022.
[29] C. Haisch, R. Niessner, O.I. Matveev, U. Panne, N. Omenetto, Element-specific determination of chlorine in gases by Laser-Induced-Breakdown-Spectroscopy (LIBS), Fresenius J. Anal. Chem. 356 (1996) 21–26.

https://doi.org/10.1007/s0021663560021.
[30] M. Gaft, L. Nagli, N. Eliezer, Y. Groisman, O. Forni, Elemental analysis of halogens using molecular emission by laser-induced breakdown spectroscopy in air, Spectrochim. Acta, Part B 98 (2014) 39–47. https://doi.org/10.1016/j.sab.2014.05.011.
[31] R.W.B. Pearse, A.G. Gaydon, The Identification of Molecular Spectra, 4th ed., Chapman and Hall Ltd., London, 1976.
[32] R.C. Johnson, T.R. Merton, The band spectra of the alkaline earth halides. I.—CaF, SrF, Proc. R. Soc. A. 122 (1929) 161–188. https://doi.org/10.1098/rspa.1929.0012.
[33] C. Álvarez, J. Pisonero, N. Bordel, Quantification of fluorite mass-content in powdered ores using a Laser-Induced Breakdown Spectroscopy method based on the detection of minor elements and CaF molecular bands, Spectrochim. Acta, Part B 100 (2014) 123–128. https://doi.org/10.1016/j.sab.2014.07.024.
[34] C. Alvarez-Llamas, J. Pisonero, N. Bordel, Quantification of fluorine traces in solid samples using CaF molecular emission bands in atmospheric air Laser-Induced Breakdown Spectroscopy, Spectrochim. Acta, Part B 123 (2016) 157–162. https://doi.org/10.1016/j.sab.2016.08.006.
[35] C. Alvarez-Llamas, J. Pisonero, N. Bordel, A novel approach for quantitative LIBS fluorine analysis using CaF emission in calcium-free samples, J. Anal. At. Spectrom. 32 (2017) 162–166. https://doi.org/10.1039/C6JA00386A.
[36] O. Forni, M. Gaft, M.J. Toplis, S.M. Clegg, S. Maurice, R.C. Wiens, N. Mangold, O. Gasnault, V. Sautter, S. Le Mouélic, P.-Y. Meslin, M. Nachon, R.E. McInroy, A.M. Ollila, A. Cousin, J.C. Bridges, N.L. Lanza, M.D. Dyar, First detection of fluorine on Mars: Implications for Gale Crater's geochemistry, Geophys. Res. Lett. 42 (2015) 1020–1028. https://doi.org/10.1002/2014GL062742.
[37] D.S. Vogt, K. Rammelkamp, S. Schröder, H.W. Hübers, Molecular emission in laser-induced breakdown spectroscopy: An investigation of its suitability for chlorine quantification on Mars, Icarus 302 (2018) 470–482. https://doi.org/10.1016/j.icarus.2017.12.006.
[38] D.S. Vogt, S. Schröder, K. Rammelkamp, P.B. Hansen, S. Kubitza, H.-W. Hübers, CaCl and CaF emission in LIBS under simulated martian conditions, Icarus 335 (2020) 113393. https://doi.org/10.1016/j.icarus.2019.113393.
[39] T. Dietz, J. Klose, P. Kohns, G. Ankerhold, Quantitative determination of chlorides by molecular laser-induced breakdown spectroscopy, Spectrochim. Acta, Part B 152 (2019) 59–67. https://doi.org/10.1016/j.sab.2018.12.009.
[40] M. Gaft, L. Nagli, R. Lezion, P. Tikva, Method of Laser-Induced Breakdown Spectroscopy in Air, US 2016/0116415 A1, 2016.
[41] M. Gaft, L. Nagli, Y. Raichlin, F. Pelascini, G. Panzer, V.M. Ros, Laser-induced breakdown spectroscopy of Br and I molecules with alkali-earth elements, Spectrochim. Acta, Part B 157 (2019) 47–52. https://doi.org/10.1016/j.sab.2019.05.003.
[42] A. Sarkar, X. Mao, G.C.-Y. Chan, R.E. Russo, Laser ablation molecular isotopic spectrometry of water for $_1D^2/_1H^1$ ratio analysis, Spectrochim. Acta, Part B 88 (2013) 46–53. https://doi.org/10.1016/j.sab.2013.08.002.
[43] A. D'Ulivo, M. Onor, E. Pitzalis, R. Spiniello, L. Lampugnani, G. Cristoforetti, S. Legnaioli, V. Palleschi, A. Salvetti, E. Tognoni, Determination of the deuterium/hydrogen ratio in gas reaction products by laser-induced breakdown spectroscopy, Spectrochim. Acta, Part B 61 (2006) 797–802. https://doi.org/10.1016/j.sab.2006.06.001.

[44] W. Pietsch, A. Petit, A. Briand, Isotope ratio determination of uranium by optical emission spectroscopy on a laser-produced plasma - basic investigations and analytical results, Spectrochim. Acta, Part B 53 (1998) 751–761. https://doi.org/10.1016/S0584-8547(97)00123-7.
[45] C.A. Smith, M.A. Martinez, D.K. Veirs, D.A. Cremers, Pu-239/Pu-240 isotope ratios determined using high resolution emission spectroscopy in a laser-induced plasma, Spectrochim. Acta, Part B 57 (2002) 929–937. https://doi.org/10.1016/S0584-8547(02)00023-X.
[46] H. Niki, T. Yasuda, I. Kitazima, Measurement Technique of Boron Isotopic Ratio by Laser-induced Breakdown Spectroscopy, J. Nucl. Sci. Technol. 35 (1998) 34–39. https://doi.org/10.1080/18811248.1998.9733817.
[47] X. Mao, A.A. Bol'shakov, I. Choi, C.P. McKay, D.L. Perry, O. Sorkhabi, R.E. Russo, Laser Ablation Molecular Isotopic Spectrometry: Strontium and its isotopes, Spectrochim. Acta, Part B 66 (2011) 767–775. https://doi.org/10.1016/j.sab.2011.12.002.
[48] X. Mao, G.C.-Y. Chan, I. Choi, V. Zorba, R.E. Russo, Combination of atomic lines and molecular bands for uranium optical isotopic analysis in laser induced plasma spectrometry, J. Radioanal. Nucl. Chem. 312 (2017) 121–131. https://doi.org/10.1007/s10967-017-5197-y.
[49] A.A. Bol'shakov, Xianglei Mao, D.L. Perry, R.E. Russo, Laser Ablation Molecular Isotopic Spectrometry for rare isotopes of the light elements, Spectroscopy 29 (2014) 30–39. https://doi.org/10.13140/2.1.3062.3364.
[50] H. Hou, G.C.-Y. Chan, X. Mao, V. Zorba, R. Zheng, R.E. Russo, Femtosecond Laser Ablation Molecular Isotopic Spectrometry for Zirconium Isotope Analysis, Anal. Chem. 87 (2015) 4788–4796. https://doi.org/10.1021/acs.analchem.5b00056.
[51] A.A. Bol'shakov, X. Mao, J.J. González, R.E. Russo, Laser ablation molecular isotopic spectrometry (LAMIS): current state of the art, J. Anal. At. Spectrom. 31 (2016) 119–134. https://doi.org/10.1039/C5JA00310E.
[52] K.C. Hartig, I. Ghebregziabher, I. Jovanovic, Standoff Detection of Uranium and its Isotopes by Femtosecond Filament Laser Ablation Molecular Isotopic Spectrometry, Sci. Rep. 7 (2017) 43852. https://doi.org/10.1038/srep43852.
[53] R. Glaus, J. Riedel, I. Gornushkin, Insight into the Formation of Molecular Species in Laser-Induced Plasma of Isotopically Labeled Organic Samples, Anal. Chem. 87 (2015) 10131–10137. https://doi.org/10.1021/acs.analchem.5b02926.
[54] H. Hou, X. Mao, V. Zorba, R.E. Russo, Laser Ablation Molecular Isotopic Spectrometry for Molecules Formation Chemistry in Femtosecond-Laser Ablated Plasmas, Anal. Chem. 89 (2017) 7750–7757. https://doi.org/10.1021/acs.analchem.7b01750.
[55] B. Welz, H. Becker-Ross, S. Florek, U. Heitmann, High-Resolution Continuum Source AAS: The Better Way to Do Atomic Absorption Spectrometry, Wiley-VCH, Weinheim, Germany, 2005.
[56] J.M. Harnly, The future of atomic absorption spectrometry: a continuum source with a charge coupled array detector?, J. Anal. At. Spectrom. 14 (1999) 137–146. https://doi.org/10.1039/a807586g.
[57] H. Becker-Roß, S. Florek, U. Heitmann, R. Weiße, Influence of the spectral bandwith of the spectrometer on the sensitivity using continuum source AAS, Fresenius J. Anal. Chem. 355 (1996) 300–303. https://doi.org/10.1007/s0021663550300.
[58] H. Becker-Ross, S.V. Florek, Echelle spectrometers and charge-coupled devices, Spectrochim. Acta, Part B 52 (1997) 1367–1375.

https://doi.org/10.1016/S0584-8547(97)00024-4.
[59] H. Becker-Ross, S. Florek, U. Heitmann, Observation, identification and correction of structured molecular background by means of continuum source AAS - determination of selenium and arsenic in human urine, J. Anal. At. Spectrom. 15 (2000) 137–141. https://doi.org/10.1039/A903571K.
[60] B. Welz, D.L.G. Borges, F.G. Lepri, M.G.R. Vale, U. Heitmann, High-resolution continuum source electrothermal atomic absorption spectrometry — An analytical and diagnostic tool for trace analysis, Spectrochim. Acta, Part B 62 (2007) 873–883. https://doi.org/10.1016/j.sab.2007.03.009.
[61] B. Welz, S. Morés, E. Carasek, M.G.R. Vale, M. Okruss, H. Becker-Ross, High-Resolution Continuum Source Atomic and Molecular Absorption Spectrometry—A Review, Appl. Spectrosc. Rev. 45 (2010) 327–354. https://doi.org/10.1080/05704928.2010.483669.
[62] M. Resano, E. García-Ruiz, High-resolution continuum source graphite furnace atomic absorption spectrometry: Is it as good as it sounds? A critical review, Anal. Bioanal. Chem. 399 (2011) 323–330. https://doi.org/10.1007/s00216-010-4105-x.
[63] M. Resano, M. Aramendia, M.A. Belarra, High-resolution continuum source graphite furnace atomic absorption spectrometry for direct analysis of solid samples and complex materials: A tutorial review, J. Anal. At. Spectrom. 29 (2014) 2229–2250. https://doi.org/10.1039/c4ja00176a.
[64] R.G.O. Araujo, B. Welz, F. Vignola, H. Becker-Ross, Correction of structured molecular background by means of high-resolution continuum source electrothermal atomic absorption spectrometry—Determination of antimony in sediment reference materials using direct solid sampling, Talanta 80 (2009) 846–852. https://doi.org/10.1016/j.talanta.2009.08.004.
[65] D.J. Butcher, Molecular absorption spectrometry in flames and furnaces: A review., Analytica Chimica Acta 804 (2013) 1–15. https://doi.org/10.1016/j.aca.2013.07.056.
[66] M. Resano, M.R. Flórez, E. García-Ruiz, Progress in the determination of metalloids and non-metals by means of high-resolution continuum source atomic or molecular absorption spectrometry. A critical review., Anal. Bioanal. Chem. 406 (2014) 2239–2259. https://doi.org/10.1007/s00216-013-7522-9.
[67] N. Ozbek, A. Baysal, Determination of sulfur by high-resolution continuum source atomic absorption spectrometry: Review of studies over the last 10 years, TrAC, Trends Anal. Chem. 88 (2017) 62–76. https://doi.org/10.1016/j.trac.2016.09.014.
[68] U. Heitmann, H. Becker-Ross, S. Florek, M.D. Huang, M. Okruss, Determination of non-metals *via* molecular absorption using high-resolution continuum source absorption spectrometry and graphite furnace atomization, J. Anal. At. Spectrom. 21 (2006) 1314–1320. https://doi.org/10.1039/b607384k.
[69] M. Resano, M.R. Flórez, Direct determination of sulfur in solid samples by means of high-resolution continuum source graphite furnace molecular absorption spectrometry using palladium nanoparticles as chemical modifier, J. Anal. At. Spectrom. 27 (2012) 401–412. https://doi.org/10.1039/c2ja10322b.
[70] H. Becker-Ross, S. Florek, U. Heitmann, M.D. Huang, M. Okruss, B. Radziuk, Continuum source atomic absorption spectrometry and detector technology: A historical perspective, Spectrochim. Acta, Part B 61 (2006) 1015–1030. https://doi.org/10.1016/j.sab.2006.09.016.
[71] M. Resano, M.R. Flórez, E. García-Ruiz, High-resolution continuum source

atomic absorption spectrometry for the simultaneous or sequential monitoring of multiple lines. A critical review of current possibilities, Spectrochim. Acta, Part B 88 (2013) 85–97. https://doi.org/10.1016/j.sab.2013.06.004.
[72] S.L.C. Ferreira, M.A. Bezerra, A.S. Santos, W.N.L. dos Santos, C.G. Novaes, O.M.C. de Oliveira, M.L. Oliveira, R.L. Garcia, Atomic absorption spectrometry – A multi element technique, TrAC, Trends Anal. Chem. 100 (2018) 1–6. https://doi.org/10.1016/j.trac.2017.12.012.
[73] S. Geisler, M. Okruss, H. Becker-Ross, M.D. Huang, N. Esser, S. Florek, Spectrometer system using a modular echelle spectrograph and a laser-driven continuum source for simultaneous multi-element determination by graphite furnace absorption spectrometry, Spectrochim. Acta, Part B 107 (2015) 11–16. https://doi.org/10.1016/j.sab.2015.02.006.
[74] V.A. Labusov, S.S. Boldova, D.O. Selunin, Z.V. Semenov, P.V. Vashchenko, S.A. Babin, High-resolution continuum-source electrothermal atomic absorption spectrometer for simultaneous multi-element determination in the spectral range of 190–780 nm, J. Anal. At. Spectrom. 34 (2019) 1005–1010. https://doi.org/10.1039/C8JA00432C.
[75] N.L.A. Jamari, A. Behrens, A. Raab, E.M. Krupp, J. Feldmann, Plasma processes to detect fluorine with ICPMS/MS as $[M–F]^+$: an argument for building a negative mode ICPMS/MS, J. Anal. At. Spectrom. 33 (2018) 1304–1309. https://doi.org/10.1039/C8JA00050F.
[76] M. Aramendía, M.R. Flórez, M. Piette, F. Vanhaecke, M. Resano, Al determination in whole blood samples as AlF via high-resolution continuum source graphite furnace molecular absorption spectrometry: potential application to forensic diagnosis of drowning, J. Anal. At. Spectrom. 26 (2011) 1964–1973. https://doi.org/10.1039/c1ja10183h.
[77] M.R. Flórez, M. Resano, Direct determination of bromine in plastic materials by means of solid sampling high-resolution continuum source graphite furnace molecular absorption spectrometry, Spectrochim. Acta, Part B 88 (2013) 32–39. https://doi.org/10.1016/j.sab.2013.07.013.
[78] U. Heitmann, B. Welz, D.L.G. Borges, F.G. Lepri, Feasibility of peak volume, side pixel and multiple peak registration in high-resolution continuum source atomic absorption spectrometry, Spectrochim. Acta, Part B 62 (2007) 1222–1230. https://doi.org/10.1016/j.sab.2007.10.011.
[79] A.L. Vieira, D.A. Gonçalves, A. Virgilio, E.C. Ferreira, B.T. Jones, G.L. Donati, J.A. Gomes Neto, Multi-energy calibration for the determination of non-metals by high-resolution continuum source molecular absorption spectrometry, J. Anal. At. Spectrom. 34 (2019) 972–978. https://doi.org/10.1039/C9JA00006B.
[80] W. Boschetti, M. Orlando, M. Dullius, M.B. Dessuy, M.G.R. Vale, B. Welz, J.B. de Andrade, Sequential and simultaneous determination of four elements in soil samples using high-resolution continuum source graphite furnace atomic and molecular absorption spectrometry, J. Anal. At. Spectrom. 31 (2016) 1269–1277. https://doi.org/10.1039/C6JA00031B.
[81] Z. Kowalewska, Feasibility of high-resolution continuum source flame molecular absorption spectrometry for silicon determination in organic solutions *via* the SiO molecule, J. Anal. At. Spectrom. 33 (2018) 260–273. https://doi.org/10.1039/C7JA00360A.
[82] H. Wiltsche, K. Prattes, M. Zischka, G. Knapp, Estimation of boron isotope ratios using high resolution continuum source atomic absorption spectrometry, Spectrochim. Acta, Part B 64 (2009) 341–346.

https://doi.org/10.1016/j.sab.2009.03.008.
[83] F.V. Nakadi, M.A.M.S. da Veiga, M. Aramendía, E. Garcia-Ruiz, M. Resano, Chlorine isotope determination *via* the monitoring of the AlCl molecule by high-resolution continuum source graphite furnace molecular absorption spectrometry - a case study, J. Anal. At. Spectrom. 30 (2015) 1531–1540. https://doi.org/10.1039/c5ja00055f.
[84] G. Herzberg, Molecular Spectra and Molecule Structure. I. Spectra of Diatomic Molecules, 2nd ed., D. Van Nostrand Company, INC., Princeton, 1950.
[85] F.V. Nakadi, M.A.M.S. da Veiga, M. Aramendía, E. Garcia-Ruiz, M. Resano, Br isotope determination *via* the monitoring of CaBr transitions using high-resolution continuum source graphite furnace molecular absorption spectrometry. Potential for direct determination of Br in solid samples using isotope dilution, J. Anal. At. Spectrom. 31 (2016) 1381–1390. https://doi.org/10.1039/c6ja00114a.
[86] C. Abad, S. Florek, H. Becker-Ross, M.-D. Huang, H.-J. Heinrich, S. Recknagel, J. Vogl, N. Jakubowski, U. Panne, Determination of boron isotope ratios by high-resolution continuum source molecular absorption spectrometry using graphite furnace vaporizers, Spectrochim. Acta, Part B 136 (2017) 116–122. https://doi.org/10.1016/j.sab.2017.08.012.
[87] M.B.T. Zanatta, F.V. Nakadi, M. Resano, M.A.M.S. da Veiga, Calcium isotope determination in urine samples via the monitoring of 44CaF and 40CaF molecules by high-resolution continuum source graphite furnace molecular absorption spectrometry, J. Anal. At. Spectrom. 34 (2019) 2280–2287. https://doi.org/10.1039/C9JA00233B.
[88] M.B.T. Zanatta, F.V. Nakadi, M.A.M.S. da Veiga, CaI and SrI molecules for iodine determination by high-resolution continuum source graphite furnace molecular absorption spectrometry: Greener molecules for practical application, Talanta 179 (2018) 563–568. https://doi.org/10.1016/j.talanta.2017.11.052.
[89] M. Schneider, B. Welz, M.-D. Huang, H. Becker-Ross, M. Okruss, E. Carasek, Iodine determination by high-resolution continuum source molecular absorption spectrometry – A comparison between potential molecules, Spectrochim. Acta, Part B 153 (2019) 42–49. https://doi.org/10.1016/j.sab.2019.01.006.
[90] A.R. Borges, L.L. François, B. Welz, E. Carasek, M.G.R. Vale, Determination of fluorine in plant materials *via* calcium mono-fluoride using high-resolution graphite furnace molecular absorption spectrometry with direct solid sample introduction, J. Anal. At. Spectrom. 29 (2014) 1564–1569. https://doi.org/10.1039/C4JA00067F.
[91] É.R. Pereira, B. Welz, A.A. Vieira, A systematic look at the carbon monosulfide molecule and chemical modifiers for the determination of sulfur by HR-CS GF MAS, J. Anal. At. Spectrom. 33 (2018) 1394–1401. https://doi.org/10.1039/C8JA00146D.
[92] M.-D. Huang, H. Becker-Ross, S. Florek, U. Heitmann, M. Okruss, B. Welz, H.S. Ferreira, High-resolution continuum source molecular absorption spectrometry of nitrogen monoxide and its application for the determination of nitrate, J. Anal. At. Spectrom. 25 (2010) 163–168. https://doi.org/10.1039/b916732c.
[93] Z. Qin, D. McNee, H. Gleisner, A. Raab, K. Kyeremeh, M. Jaspars, E. Krupp, H. Deng, J. Feldmann, Fluorine Speciation Analysis Using Reverse Phase Liquid Chromatography Coupled Off-Line to Continuum Source Molecular Absorption Spectrometry (CS-MAS): Identification and Quantification of Novel Fluorinated Organic Compounds in Environmental and Biological Samples, Anal. Chem. 84 (2012) 6213–6219. https://doi.org/10.1021/ac301201y.
[94] L.F.C. Gouvêa, A.J. Moreira, C.D. Freschi, G.P.G. Freschi, Speciation of

nitrite, nitrate and p-nitrophenol by photochemical vapor generation of NO using High-Resolution Continuum Source Molecular Absorption Spectrometry, J. Food Compos. Anal. 70 (2018) 28–34. https://doi.org/10.1016/j.jfca.2018.04.003.
[95] M.-D. Huang, H. Becker-Ross, S. Florek, U. Heitmann, M. Okruss, C.-D. Patz, Determination of sulfur forms in wine including free and total sulfur dioxide based on molecular absorption of carbon monosulfide in the air–acetylene flame, Anal. Bioanal. Chem. 390 (2008) 361–367. https://doi.org/10.1007/s00216-007-1669-1.
[96] S.D. Tanner, Characterization of ionization and matrix suppression in inductively coupled 'cold' plasma mass spectrometry, J. Anal. At. Spectrom. 10 (1995) 905–921. https://doi.org/10.1039/JA9951000905.
[97] R.F.J. Dams, J. Goossens, L. Moens, Spectral and non-spectral interferences in inductively coupled plasma mass-spectrometry, Microchim. Acta 119 (1995) 277–286. https://doi.org/10.1007/BF01244007.
[98] N. Jakubowski, L. Moens, F. Vanhaecke, Sector field mass spectrometers in ICP-MS, Spectrochim. Acta, Part B 53 (1998) 1739–1763.
[99] S.D. Tanner, V.I. Baranov, D.R. Bandura, Reaction cells and collision cells for ICP-MS: a tutorial review, Spectrochim. Acta, Part B 57 (2002) 1361–1452.
[100] T.-S. Lum, K.S.-Y. Leung, Strategies to overcome spectral interference in ICP-MS detection, J. Anal. At. Spectrom. 31 (2016) 1078–1088. https://doi.org/10.1039/C5JA00497G.
[101] P. Turner, T. Merren, J. Speakman, C. Haines, Interface studies in the ICP-mass spectrometer, in: G. Holland, S.D. Tanner (Eds.), Plasma Source Mass Spectrometry: Developments and Applications, The Royal Society of Chemistry, Cambridge, 1997: pp. 28–34.
[102] G.C. Eiden, C.J. Barinaga, D.W. Koppenaal, Beneficial Ion/Molecule Reactions in Elemental Mass Spectrometry, Rapid Commun. Mass Spectrom. 11 (1997) 37–42. https://doi.org/10.1002/(SICI)1097-0231(19970115)11:1<37::AID-RCM815>3.0.CO;2-C.
[103] U.S. EPA, Method 200.8: Determination of Trace Elements in Waters and Wastes by Inductively Coupled Plasma-Mass Spectrometry, Revision 5.4., Cincinnati, 1994. https://www.epa.gov/sites/production/files/2015-08/documents/method_200-8_rev_5-4_1994.pdf (accessed December 18, 2019).
[104] J.W. Olesik, D.R. Jones, Strategies to develop methods using ion-molecule reactions in a quadrupole reaction cell to overcome spectral overlaps in inductively coupled plasma mass spectrometry, J. Anal. At. Spectrom. 21 (2006) 141–159. https://doi.org/10.1039/B511464K.
[105] N. Yamada, Kinetic energy discrimination in collision/reaction cell ICP-MS: Theoretical review of principles and limitations, Spectrochim. Acta, Part B 110 (2015) 31–44. https://doi.org/10.1016/j.sab.2015.05.008.
[106] D.R. Bandura, V.I. Baranov, S.D. Tanner, Reaction chemistry and collisional processes in multipole devices for resolving isobaric interferences in ICP–MS, Fresenius J. Anal. Chem. 370 (2001) 454–470. https://doi.org/10.1007/s002160100869.
[107] J.T. Rowan, R.S. Houk, Attenuation of Polyatomic Ion Interferences in Inductively Coupled Plasma Mass Spectrometry by Gas-Phase Collisions, Appl. Spectrosc. 43 (1989) 976–980. https://doi.org/10.1366/0003702894204065.
[108] G.K. Koyanagi, V.I. Baranov, S.D. Tanner, D.K. Bohme, An inductively coupled plasma/selected-ion flow tube mass spectrometric study of the chemical resolution of isobaric interferences, J. Anal. At. Spectrom. 15 (2000) 1207–1210. https://doi.org/10.1039/B000989J.

[109] D.K. Böhme, Experimental studies of positive ion chemistry with flow-tube mass spectrometry: birth, evolution, and achievements in the 20th century, Int. J. Mass Spectrom. 200 (2000) 97–136. https://doi.org/10.1016/S1387-3806(00)00299-2.
[110] E.R. Denoyer, S.D. Tanner, U. Vollkopf, A new dynamic reaction cell for reducing ICP-MS interferences using chemical resolution, Spectroscopy 14 (1999) 43–54.
[111] L. Balcaen, E. Bolea-Fernandez, M. Resano, F. Vanhaecke, Inductively coupled plasma - Tandem mass spectrometry (ICP-MS/MS): A powerful and universal tool for the interference-free determination of (ultra)trace elements – A tutorial review, Anal. Chim. Acta 894 (2015) 7–19. https://doi.org/10.1016/j.aca.2015.08.053.
[112] E. Bolea-Fernández, L. Balcaen, M. Resano, F. Vanhaecke, Overcoming spectral overlap *via* inductively coupled plasma-tandem mass spectrometry (ICP-MS/MS). A tutorial review, J. Anal. At. Spectrom. 32 (2017) 1660–1679. https://doi.org/10.1039/c7ja00010c.
[113] S. D'Ilio, N. Violante, C. Majorani, F. Petrucci, Dynamic reaction cell ICP-MS for determination of total As, Cr, Se and V in complex matrices: Still a challenge? A review, Anal. Chim. Acta 698 (2011) 6–13. https://doi.org/10.1016/j.aca.2011.04.052.
[114] G.K. Koyanagi, D. Caraiman, V. Blagojevic, D.K. Bohme, Gas-Phase Reactions of Transition-Metal Ions with Molecular Oxygen: Room-Temperature Kinetics and Periodicities in Reactivity, J. Phys. Chem. A 106 (2002) 4581–4590. https://doi.org/10.1021/jp014145j.
[115] T. Narukawa, K. Chiba, Oxygenation Mechanism of Ions in Dynamic Reaction Cell ICP-MS, Anal. Sci. 29 (2013) 747–752. https://doi.org/10.2116/analsci.29.747.
[116] D.R. Bandura, V.I. Baranov, S.D. Tanner, Inductively coupled plasma mass spectrometer with axial field in a quadrupole reaction cell, J. Am. Soc. Spectrom. 13 (2002) 1176–1185. https://doi.org/10.1016/S1044-0305(02)00435-X.
[117] V.I. Baranov, S.D. Tanner, A dynamic reaction cell for inductively coupled plasma mass spectrometry (ICP-DRC-MS). Part 1. The rf-field energy contribution in thermodynamics of ion-molecule reactions, J. Anal. At. Spectrom. 14 (1999) 1133–1142. https://doi.org/10.1039/A809889A.
[118] S.D. Tanner, V.I. Baranov, Theory, Design, and Operation of a Dynamic Reaction Cell for ICP-MS, At. Spectrosc. 20 (1999) 45–52.
[119] S.D. Tanner, V.I. Baranov, A dynamic reaction cell for inductively coupled plasma mass spectrometry (ICP-DRC-MS). II. Reduction of interferences produced within the cell, J. Am. Soc. Mass Spectrom. 10 (1999) 1083–1094. https://doi.org/10.1016/S1044-0305(99)00081-1.
[120] S.D. Tanner, V.I. Baranov, U. Vollkopf, A dynamic reaction cell for inductively coupled plasma mass spectrometry (ICP-DRC-MS). Part III. Optimization and analytical performance, J. Anal. At. Spectrom. 15 (2000) 1261–1269. https://doi.org/10.1039/b002604m.
[121] D.R. Bandura, V.I. Baranov, S.D. Tanner, Detection of Ultratrace Phosphorus and Sulfur by Quadrupole ICPMS with Dynamic Reaction Cell, Anal. Chem. 74 (2002) 1497–1502. https://doi.org/10.1021/ac011031v.
[122] S. Diez Fernández, N. Sugishama, J. Ruiz Encinar, A. Sanz-Medel, Triple Quad ICPMS (ICPQQQ) as a New Tool for Absolute Quantitative Proteomics and Phosphoproteomics, Anal. Chem. 84 (2012) 5851–5857. https://doi.org/10.1021/ac3009516.
[123] L. Balcaen, G. Woods, M. Resano, F. Vanhaecke, Accurate determination of S

in organic matrices using isotope dilution ICP-MS/MS, J. Anal. At. Spectrom. 28 (2013) 33–39. https://doi.org/10.1039/C2JA30265A.
[124] R.S. Amais, C.D.B. Amaral, L.L. Fialho, D. Schiavo, J.A. Nóbrega, Determination of P, S and Si in biodiesel, diesel and lubricating oil using ICP-MS/MS, Anal. Methods 6 (2014) 4516–4520. https://doi.org/10.1039/C4AY00279B.
[125] J. Nelson, H. Hopfer, F. Silva, S. Wilbur, J. Chen, K.S. Ozawa, P.L. Wylie, Evaluation of GC-ICP-MS/MS as a New Strategy for Specific Heteroatom Detection of Phosphorus, Sulfur, and Chlorine Determination in Foods, J. Agric. Food Chem. 63 (2015) 4478–4483. https://doi.org/10.1021/jf506372e.
[126] B. Lajin, W. Goessler, Sulfur speciation by HPLC-ICPQQQMS in complex human biological samples: taurine and sulfate in human serum and urine, Anal. Bioanal. Chem. 410 (2018) 6787–6793. https://doi.org/10.1007/s00216-018-1251-z.
[127] D.P. Bishop, D. Clases, F. Fryer, E. Williams, S. Wilkins, D.J. Hare, N. Cole, U. Karst, P.A. Doble, Elemental bio-imaging using laser ablation-triple quadrupole-ICP-MS, J. Anal. At. Spectrom. 31 (2016) 197–202. https://doi.org/10.1039/C5JA00293A.
[128] S. Meyer, A. López-Serrano, H. Mitze, N. Jakubowski, T. Schwerdtle, Single-cell analysis by ICP-MS/MS as a fast tool for cellular bioavailability studies of arsenite, Metallomics 10 (2018) 73–76. https://doi.org/10.1039/c7mt00285h.
[129] I. Feldmann, N. Jakubowski, D. Stuewer, Application of a hexapole collision and reaction cell in ICP-MS Part I: Instrumental aspects and operational optimization, Fresenius J. Anal. Chem. 365 (1999) 415–421. https://doi.org/10.1007/s002160051633.
[130] L. Somoano-Blanco, P. Rodríguez-González, D. Pröfrock, A. Prange, J.I.G. Alonso, Comparison of different mass spectrometric techniques for the determination of polychlorinated biphenyls by isotope dilution using ^{37}Cl-labelled analogues, Anal. Methods 7 (2015) 9068–9075. https://doi.org/10.1039/C5AY01752A.
[131] B. Klencsár, E. Bolea-Fernandez, M.R. Flórez, L. Balcaen, F. Cuyckens, F. Lynen, F. Vanhaecke, Determination of the total drug-related chlorine and bromine contents in human blood plasma using high performance liquid chromatography-tandem ICP-mass spectrometry (HPLC-ICP-MS/MS), J. Pharm. Biomed. Anal. 124 (2016) 112–119. https://doi.org/10.1016/j.jpba.2016.02.019.
[132] L. Balcaen, E. Bolea-Fernandez, M. Resano, F. Vanhaecke, Accurate determination of ultra-trace levels of Ti in blood serum using ICP-MS/MS, Anal. Chim. Acta 809 (2014) 1–8. https://doi.org/10.1016/j.aca.2013.10.017.
[133] K.J. Hogmalm, T. Zack, A.K.-O. Karlsson, A.S.L. Sjöqvist, D. Garbe-Schönberg, *In situ* Rb–Sr and K–Ca dating by LA-ICP-MS/MS: an evaluation of N_2O and SF_6 as reaction gases, J. Anal. At. Spectrom. 32 (2017) 305–313. https://doi.org/10.1039/C6JA00362A.
[134] E. Bolea-Fernandez, L. Balcaen, M. Resano, F. Vanhaecke, Tandem ICP-mass spectrometry for Sr isotopic analysis without prior Rb/Sr separation, J. Anal. At. Spectrom. 31 (2015) 303–310. https://doi.org/10.1039/C5JA00157A.
[135] E. Bolea-Fernandez, S.J.M.V. Malderen, L. Balcaen, M. Resano, F. Vanhaecke, Laser ablation-tandem ICP-mass spectrometry (LA-ICP-MS/MS) for direct Sr isotopic analysis of solid samples with high Rb/Sr ratios, J. Anal. At. Spectrom. 31 (2016) 464–472. https://doi.org/10.1039/C5JA00404G.
[136] N. Nonose, M. Ohata, T. Narukawa, A. Hioki, K. Chiba, Removal of isobaric interferences in isotope dilution analysis of vanadium in silicon nitride fine ceramics powder by DRC-ICP-MS, J. Anal. At. Spectrom. 24 (2009) 310–319. https://doi.org/10.1039/B812565A.

[137] M. Yamanaka, S. Wilbur, Accurate Determination of TiO2 Nanoparticles in Complex Matrices using the Agilent 8900 ICP-QQQ, Publication Number 5991-8358EN. (2017) 7.
[138] A. Virgilio, D.A. Gonçalves, T. McSweeney, J.A. Gomes Neto, J.A. Nóbrega, G.L. Donati, Multi-energy calibration applied to atomic spectrometry, Anal. Chim. Acta 982 (2017) 31–36. https://doi.org/10.1016/j.aca.2017.06.040.
[139] E. Bolea-Fernandez, L. Balcaen, M. Resano, F. Vanhaecke, Potential of Methyl Fluoride as a Universal Reaction Gas to Overcome Spectral Interference in the Determination of Ultratrace Concentrations of Metals in Biofluids Using Inductively Coupled Plasma-Tandem Mass Spectrometry, Anal. Chem. 86 (2014) 7969–7977. https://doi.org/10.1021/ac502023h.
[140] E. Bolea-Fernández, K. Phan, L. Balcaen, M. Resano, F. Vanhaecke, Determination of ultra-trace amounts of prosthesis-related metals in whole blood using volumetric absorptive micro-sampling and tandem ICP - Mass spectrometry, Anal. Chim. Acta 941 (2016) 1–9. https://doi.org/10.1016/j.aca.2016.08.030.
[141] N.L.A. Jamari, J.F. Dohmann, A. Raab, E.M. Krupp, J. Feldmann, Novel non-target analysis of fluorine compounds using ICPMS/MS and HPLC-ICPMS/MS, J. Anal. At. Spectrom. 32 (2017) 942–950. https://doi.org/10.1039/C7JA00051K.
[142] C.B. Williams, G.L. Donati, Multispecies calibration: a novel application for inductively coupled plasma tandem mass spectrometry, J. Anal. At. Spectrom. 33 (2018) 762–767. https://doi.org/10.1039/C8JA00034D.
[143] G.L. Donati, R.S. Amais, Fundamentals and new approaches to calibration in atomic spectrometry, J. Anal. At. Spectrom. 34 (2019) 2353–2369. https://doi.org/10.1039/C9JA00273A.
[144] A. Virgilio, J.A. Nóbrega, G.L. Donati, Multi-isotope calibration for inductively coupled plasma mass spectrometry, Anal. Bioanal. Chem. 410 (2018) 1157–1162. https://doi.org/10.1007/s00216-017-0753-4.
[145] Q. He, J. Wu, S. Zhang, X. Fang, Z. Xing, C. Wei, X. Zhang, Rapid screening of gaseous catalysts in methane activation using ICP-QQQ-MS, J. Anal. At. Spectrom. 33 (2018) 563–568. https://doi.org/10.1039/C7JA00345E.
[146] L. Moens, N. Jakubowski, The only general method for overcoming spectroscopic interference requires double-focusing instrumentation.: Double-Focusing Mass Spectrometers in ICPMS, Anal. Chem. 70 (1998) 251A-256A. https://doi.org/10.1021/ac9818069.
[147] E. Bolea-Fernández, D. Leite, A. Rua-Ibarz, T. Liu, G. Woods, M. Aramendia, M. Resano, F. Vanhaecke, On the effect of using collision/reaction cell (CRC) technology in single-particle ICP-mass spectrometry (SP-ICP-MS)., Anal. Chim. Acta 1077 (2019) 95–106. https://doi.org/10.1016/j.aca.2019.05.077.
[148] M. Bonta, J.J. Gonzalez, C.D. Quarles Jr., R.E. Russo, B. Hegedus, A. Limbeck, Elemental mapping of biological samples by the combined use of LIBS and LA-ICP-MS, J. Anal. At. Spectrom. 31 (2016) 252–258. https://doi.org/10.1039/C5JA00287G.
[149] N. Turhan, N. Ozbek, S. Akman, Method development for the determination of bromine *via* molecular absorption of barium monobromide by high-resolution continuum source molecular absorption spectrometry, J. Anal. At. Spectrom. 34 (2019) 577–582. https://doi.org/10.1039/C8JA00422F.
[150] M.D. Huang, H. Becker-Ross, S. Florek, U. Heitmann, M. Okruss, High-resolution continuum source electrothermal absorption spectrometry of AlBr and CaBr for the determination of bromine, Spectrochim. Acta, Part B 63 (2008) 566–570. https://doi.org/10.1016/j.sab.2008.02.005.

[151] F. Cacho, L. Machynak, M. Nemecek, E. Beinrohr, Determination of bromide in aqueous solutions via the TlBr molecule using high-resolution continuum source graphite furnace molecular absorption spectrometry, Spectrochim. Acta, Part B 144 (2018) 63–67. https://doi.org/10.1016/j.sab.2018.03.010.
[152] M.D. Huang, H. Becker-Ross, S. Florek, U. Heitmann, M. Okruss, Determination of halogens *via* molecules in the air–acetylene flame using high-resolution continuum source absorption spectrometry, Part II: Chlorine, Spectrochim. Acta, Part B 61 (2006) 959–964. https://doi.org/10.1016/j.sab.2006.08.004.
[153] M.S.P. Enders, A.O. Gomes, R.F. Oliveira, R.C.L. Guimarães, M.F. Mesko, E.M.M. Flores, E.I. Müller, Determination of Chlorine in Crude Oil by High-Resolution Continuum Source Graphite Furnace Molecular Absorption Spectrometry Using AlCl, InCl, and SrCl Molecules, Energy Fuels 30 (2016) 3637–3643. https://doi.org/10.1021/acs.energyfuels.5b02100.
[154] A. Guarda, M. Aramendia, I. Andrés, E. García-Ruiz, P.C. do Nascimento, M. Resano, Determination of chlorine via the CaCl molecule by high-resolution continuum source graphite furnace molecular absorption spectrometry and direct solid sample analysis., Talanta 162 (2017) 354–361. https://doi.org/10.1016/j.talanta.2016.10.039.
[155] H. Tinas, S. Akman, Method development for the determination of chlorine by high-resolution graphite furnace molecular absorption spectrometry via GaCl, Spectrochim. Acta, Part B 148 (2018) 60–64. https://doi.org/10.1016/j.sab.2018.06.003.
[156] R.L.S. Medeiros, S.O. Souza, R.G.O. Araújo, D.R. da Silva, T.A. Maranhão, Chlorine determination via MgCl molecule in environmental samples using high resolution continuum source graphite furnace molecular absorption spectrometry, Talanta 176 (2018) 227–233. https://doi.org/10.1016/j.talanta.2017.08.026.
[157] É.R. Pereira, L.M. Rocha, H.R. Cadorim, V.D. Silva, B. Welz, E. Carasek, J.B. de Andrade, Determination of chlorine in coal via the SrCl molecule using high-resolution graphite furnace molecular absorption spectrometry and direct solid sample analysis, Spectrochim. Acta, Part B 114 (2015) 46–50. https://doi.org/10.1016/j.sab.2015.10.001.
[158] M.D. Huang, H. Becker-Ross, S. Florek, U. Heitmann, M. Okruss, Determination of halogens *via* molecules in the air–acetylene flame using high-resolution continuum source absorption spectrometry: Part I. Fluorine, Spectrochim. Acta, Part B 61 (2006) 572–578. https://doi.org/10.1016/j.sab.2006.04.007.
[159] N. Ozbek, S. Akman, Method development for the determination of fluorine in toothpaste via molecular absorption of aluminum mono fluoride using a high-resolution continuum source nitrous oxide/acetylene flame atomic absorption spectrophotometer, Talanta 94 (2012) 246–250. https://doi.org/10.1016/j.talanta.2012.03.034.
[160] S. Morés, G.C. Monteiro, F.S. Santos, E. Carasek, B. Welz, Determination of fluorine in tea using high-resolution molecular absorption spectrometry with electrothermal vaporization of the calcium mono-fluoride CaF, Talanta 85 (2011) 2681–2685. https://doi.org/10.1016/j.talanta.2011.08.044.
[161] N. Ozbek, S. Akman, Method development for the determination of fluorine in water samples via the molecular absorption of strontium monofluoride formed in an electrothermal atomizer, Spectrochim. Acta, Part B 69 (2012) 32–37. https://doi.org/10.1016/j.sab.2012.03.003.
[162] S. Bücker, J. Acker, Spectrometric analysis of process etching solutions of the photovoltaic industry–determination of HNO_3, HF, and H_2SiF_6 using high-resolution

continuum source absorption spectrometry of diatomic molecules and atoms., Talanta 94 (2012) 335–341. https://doi.org/10.1016/j.talanta.2012.03.052.
[163] R.B. Ferreira, S.R. Oliveira, V.P. Franzini, A. Virgilio, J.L. Raposo Jr., J.A. Gomes Neto, Evaluation of Lines of Phosphorus and Potassium by High-Resolution Continuum Source Flame Atomic Absorption Spectrometry for Liquid Fertilizer Analysis, At. Spectrosc. 32 (2011) 56–61.
[164] M.A. Bechlin, J.A. Gomes Neto, J.A. Nóbrega, Evaluation of lines of boron, phosphorus and sulfur by high-resolution continuum source flame atomic absorption spectrometry for plant analysis, Microchem. J. 109 (2012) 134–138. https://doi.org/10.1016/j.microc.2012.03.013.
[165] M. Resano, J. Briceño, M.A. Belarra, Direct determination of phosphorus in biological samples using a solid sampling-high resolution-continuum source electrothermal spectrometer: comparison of atomic and molecular absorption spectrometry, J. Anal. At. Spectrom. 24 (2009) 1343–1354. https://doi.org/10.1039/b907937h.
[166] M.-D. Huang, H. Becker-Ross, M. Okruss, S. Geisler, S. Florek, Determination of phosphorus using high-resolution diphosphorus molecular absorption spectra produced in the graphite furnace, Spectrochim. Acta, Part B 115 (2016) 23–30. https://doi.org/10.1016/j.sab.2015.10.007.
[167] M.D. Huang, H. Becker-Ross, S. Florek, U. Heitmann, M. Okruss, Determination of sulfur by molecular absorption of carbon monosulfide using a high-resolution continuum source absorption spectrometer and an air-acetylene flame, Spectrochim. Acta, Part B 61 (2006) 181–188. https://doi.org/10.1016/j.sab.2006.01.001.
[168] A. Virgilio, J.L. Raposo Jr., A.A. Cardoso, J.A. Nóbrega, J.A. Gomes Neto, Determination of Total Sulfur in Agricultural Samples by High-Resolution Continuum Source Flame Molecular Absorption Spectrometry, J. Agric. Food Chem. 59 (2011) 2197–2201. https://doi.org/10.1021/jf104296d.
[169] H.R. Cadorim, É.R. Pereira, E. Carasek, B. Welz, J.O.B. de Andrade, Determination of sulfur in crude oil using high-resolution continuum source molecular absorption spectrometry of the SnS molecule in a graphite furnace, Talanta 146 (2016) 203–208. https://doi.org/10.1016/j.talanta.2015.07.088.
[170] M.D. Huang, H. Becker-Ross, S. Florek, C. Abad, M. Okruss, Investigation of high-resolution absorption spectra of diatomic sulfides of group 14 elements in graphite furnace and the comparison of their performance for sulfur determination, Spectrochim. Acta, Part B 135 (2017) 15–21. https://doi.org/10.1016/j.sab.2017.06.012.
[171] N. Sugiyama, Y. Shikamori, Analysis of Drug Active Pharmaceutical Ingredients and Biomolecules Using Triple Quadrupole ICP-MS, in: Y. Ogra, T. Hirata (Eds.), Metallomics: Recent Analytical Techniques and Applications, Springer, Tokyo, 2017. https://doi.org/10.1007/978-4-431-56463-8.
[172] B. Klencsár, C. Sánchez, L. Balcaen, J. Todolí, F. Lynen, F. Vanhaecke, Comparative evaluation of ICP sample introduction systems to be used in the metabolite profiling of chlorine-containing pharmaceuticals via HPLC-ICP-MS, J. Pharm. Biomed. Anal. 153 (2018) 135–144. https://doi.org/10.1016/j.jpba.2018.02.031.
[173] J. Nelson, L. Poirier, F. Lopez-Linares, Determination of chloride in crude oils by direct dilution using inductively coupled plasma tandem mass spectrometry (ICP-MS/MS), J. Anal. At. Spectrom. 34 (2019) 1433–1438. https://doi.org/10.1039/C9JA00096H.

[174] J. Gong, M.J. Solivio, E.J. Merino, J.A. Caruso, J.A. Landero-Figueroa, Developing ICP-MS/MS for the detection and determination of synthetic DNA-protein crosslink models via phosphorus and sulfur detection, Anal. Bioanal. Chem. 407 (2015) 2433–2437. https://doi.org/10.1007/s00216-015-8504-x.
[175] G. Hermann, L.H. Møller, B. Gammelgaard, J. Hohlweg, D. Mattanovich, S. Hann, G. Koellensperger, *In vivo* synthesized ^{34}S enriched amino acid standards for species specific isotope dilution of proteins, J. Anal. At. Spectrom. 31 (2016) 1830–1835. https://doi.org/10.1039/C6JA00039H.
[176] F. Calderón-Celis, S. Diez-Fernández, J.M. Costa-Fernández, J.R. Encinar, J.J. Calvete, A. Sanz-Medel, Elemental Mass Spectrometry for Absolute Intact Protein Quantification without Protein-Specific Standards: Application to Snake Venomics, Anal. Chem. 88 (2016) 9699–9706. https://doi.org/10.1021/acs.analchem.6b02585.
[177] X. Wang, J. Liu, X. Wang, B. Shao, L. Liu, J. Zhang, Direct quantification of total sulfur dioxide in wine using triple quadrupole ICP-MS, Anal. Methods 7 (2015) 3224–3228. https://doi.org/10.1039/C4AY02863E.
[178] B. Lajin, W. Goessler, Exploring the sulfur species in wine by HPLC-ICPMS/MS, Anal. Chim. Acta 1092 (2019) 1–8. https://doi.org/10.1016/j.aca.2019.09.074.
[179] M. Menendez-Miranda, M.T. Fernandez-Arguelles, J.M. Costa-Fernandez, J.R. Encinar, A. Sanz-Medel, Elemental ratios for characterization of quantum-dots populations in complex mixtures by asymmetrical flow field-flow fractionation on-line coupled to fluorescence and inductively coupled plasma mass spectrometry, Anal. Chim. Acta 839 (2014) 8–13. https://doi.org/10.1016/j.aca.2014.06.034.
[180] S. Musil, Á.H. Pétursdóttir, A. Raab, H. Gunnlaugsdóttir, E. Krupp, J. Feldmann, Speciation Without Chromatography Using Selective Hydride Generation: Inorganic Arsenic in Rice and Samples of Marine Origin, Anal. Chem. 86 (2014) 993–999. https://doi.org/10.1021/ac403438c.
[181] S. Meyer, M. Matissek, S.M. Müller, M.S. Taleshi, F. Ebert, K.A. Francesconi, T. Schwerdtle, *In vitro* toxicological characterisation of three arsenic-containing hydrocarbons, Metallomics 6 (2014) 1023–1033. https://doi.org/10.1039/c4mt00061g.
[182] Á.H. Pétursdóttir, N. Friedrich, S. Musil, A. Raab, H. Gunnlaugsdóttir, E.M. Krupp, J. Feldmann, Hydride generation ICP-MS as a simple method for determination of inorganic arsenic in rice for routine biomonitoring, Anal. Methods 6 (2014) 5392–5396. https://doi.org/10.1039/C4AY00423J.
[183] B.P. Jackson, Fast ion chromatography-ICP-QQQ for arsenic speciation, J. Anal. At. Spectrom. 30 (2015) 1405–1407. https://doi.org/10.1039/C5JA00049A.
[184] B.P. Jackson, A. Liba, J. Nelson, Advantages of reaction cell ICP-MS on doubly charged interferences for arsenic and selenium analysis in foods, J. Anal. At. Spectrom. 30 (2015) 1179–1183. https://doi.org/10.1039/C4JA00310A.
[185] É.R. Pereira, J.F. Kopp, A. Raab, E.M. Krupp, J. del C. Menoyo, E. Carasek, B. Welz, J. Feldmann, Arsenic containing medium and long chain fatty acids in marine fish oil identified as degradation products using reversed-phase HPLC-ICP-MS/ESI-MS, J. Anal. At. Spectrom. 31 (2016) 1836–1845. https://doi.org/10.1039/C6JA00162A.
[186] A. Gourgiotis, T. Ducasse, E. Barker, P. Jollivet, S. Gin, S. Bassot, C. Cazala, Silicon isotope ratio measurements by inductively coupled plasma tandem mass spectrometry for alteration studies of nuclear waste glasses, Anal. Chim. Acta 954 (2017) 68–76. https://doi.org/10.1016/j.aca.2016.11.063.
[187] R.S. Amais, A. Virgilio, D. Schiavo, J.A. Nóbrega, Tandem mass spectrometry

(ICP-MS/MS) for overcoming molybdenum oxide interferences on Cd determination in milk, Microchem. J. 120 (2015) 64–68. https://doi.org/10.1016/j.microc.2015.01.008.
[188] F.M. Wærsted, K.A. Jensen, E. Reinoso-Maset, L. Skipperud, High Throughput, Direct Determination of ^{226}Ra in Water and Digested Geological Samples, Anal. Chem. 90 (2018) 12246–12252. https://doi.org/10.1021/acs.analchem.8b03494.
[189] A.M. Cruz-Uribe, R. Mertz-Kraus, T. Zack, M.D. Feineman, G. Woods, D.E. Jacob, A New LA-ICP-MS Method for Ti in Quartz: Implications and Application to High Pressure Rutile-Quartz Veins from the Czech Erzgebirge, Geostand. Geoanal. Res. 41 (2017) 29–40. https://doi.org/10.1111/ggr.12132.
[190] N. Sugiyama, Y. Shikamori, Removal of spectral interferences on noble metal elements using MS/MS reaction cell mode of a triple quadrupole ICP-MS, J. Anal. At. Spectrom. 30 (2015) 2481–2487. https://doi.org/10.1039/C5JA00308C.
[191] J. Soto-Alvaredo, F. Dutschke, J. Bettmer, M. Montes-Bayón, D. Pröfrock, A. Prange, Initial results on the coupling of sedimentation field-flow fractionation (SdFFF) to inductively coupled plasma-tandem mass spectrometry (ICP-MS/MS) for the detection and characterization of TiO_2 nanoparticles, J. Anal. At. Spectrom. 31 (2016) 1549–1555. https://doi.org/10.1039/C6JA00079G.
[192] C. Walkner, R. Gratzer, T. Meisel, S.N.H. Bokhari, Multi-element analysis of crude oils using ICP-QQQ-MS, Org. Geochem. 103 (2017) 22–30. https://doi.org/10.1016/j.orggeochem.2016.10.009.
[193] T. Suoranta, S.N.H. Bokhari, T. Meisel, M. Niemelä, P. Perämäki, Elimination of Interferences in the Determination of Palladium, Platinum and Rhodium Mass Fractions in Moss Samples using ICP-MS/MS, Geostand. Geoanal. Res. 40 (2016) 559–569. https://doi.org/10.1111/ggr.12116.
[194] E. Bolea-Fernandez, L. Balcaen, M. Resano, F. Vanhaecke, Interference-free determination of ultra-trace concentrations of arsenic and selenium using methyl fluoride as a reaction gas in ICP-MS/MS, Anal. Bioanal. Chem. 407 (2015) 919–929. https://doi.org/10.1007/s00216-014-8195-8.
[195] K. Folens, T. Van Acker, E. Bolea-Fernández, G. Cornelis, F. Vanhaecke, G. Du Laing, S. Rauch, Identification of platinum nanoparticles in road dust leachate by single particle inductively coupled plasma-mass spectrometry, Sci. Total Environ. 615 (2018) 849–856. https://doi.org/10.1016/j.scitotenv.2017.09.285.

Highlights

- Elemental analysis benefits from monitoring highly resolved molecular spectra
- New possibilities for isotopic analysis using optical methods are discussed
- Producing and measuring polyatomic species in ICP-MS/MS improves selectivity
- Applications of the most representative atomic techniques are highlighted

Declaration of interests

☒ The authors declare that they have no known competing financial interests or personal relationships that could have appeared to influence the work reported in this paper.

☐The authors declare the following financial interests/personal relationships which may be considered as potential competing interests: